DR. AZHARUDDIN SAJID SYED KHAJA (Orcid ID : 0000-0003-1594-1826)

DR. JULIUS SEMENAS (Orcid ID : 0000-0001-5394-7239)

PROF. JENNY LIAO PERSSON (Orcid ID : 0000-0001-7682-7678)

Received Date : 07-Jul-2021

Revised Date : 23-Nov-2021

Accepted Date : 02-Dec-2021

Article type : Research Article

FcγRIIIa receptor interacts with androgen receptor and PIP5K1α to promote growth and metastasis of prostate cancer

Per Flodbring Larsson[1,#], Richard Karlsson[1,2,#], Martuza Sarwar[1], Regina Miftakhova[1], Tianyan Wang[1], Azharuddin Sajid Syed Khaja[1], Julius Semenas[1], Sa Chen[1], Andreas Hedblom[1,2], Amjad Ali[1], Kristina Ekström-Holka[3], Athanasios Simoulis[4], Anjani Kumar[1], Anette Gjörloff Wingren[5], Brian Robinson[6], Sun Nyunt Wai[1,7], Nigel P Mongan[8], David M Heery[9], Daniel Öhlund[10], Thomas Grundström[1], Niels Ødum[11], Jenny L Persson[1,2,5*]

[1]Department of Molecular Biology, Umeå University, Umeå, Swede, [2]Division of Experimental Cancer Research, Department of Translational Medicine, Lund University, Clinical Research Centre, Malmö Sweden. [3]Center for Molecular Pathology, Lund University, and [4]Department of Clinical Pathology and Cytology, Skåne University Hospital, Malmö, Sweden. [5]Faculty of

Biomedicine, Malmö University, Malmö, Sweden, [6]Department of Pathology, Weill Cornell Medical College, New York, NY, USA. [7]Umeå Centre for Microbial Research (UCMR), Umeå University, Umeå, Sweden.[8]Faculty of Medicine and Health Sciences, School of Veterinary Medicine and Sciences and [9]School of Pharmacy, University of Nottingham, Nottingham, United Kingdom. [10]Wallenberg Centre for Molecular Medicine, and Department of Radiation Sciences, Umeå University, Umeå, Sweden. [11]Department of Immunology and Microbiology, University of Copenhagen, Copenhagen, Denmark.

[#]shared first authorship

*****Correspondence author: Jenny L. Persson, Department of Molecular Biology, Umeå University, 901 87 Umeå, Sweden. Tel: +46-706391199. E-mail: jenny.persson@umu.se

Abbreviations: PCa: prostate cancer; BPH: benign prostate hyperplasia; CRPC: castration-resistant prostate cancer; BRFS: biochemical recurrence-free survival; FcγRIIIa: low affinity immunoglobulin gamma Fc region receptor III-A; AR: Androgen receptor; DHT: Dihydrotestosterone; PIP5K1α: Phosphatidylinositol 4-phosphate 5-kinase type-1 alpha; PIP2: phosphatidylinositol 4,5-P_2; ALDH: Aldehyde dehydrogenases; ARE-Luc vector: androgen responsive element luciferase vector; GDPR: The General Data Protection Regulation.

Key Words: prostate cancer metastasis, targeted therapy, FcγRIIIa receptor, PIP5K1α, AR pathway and antibody-based therapy.

Running title: Role of FcγRIIIa in PCa progression and metastasis.

Abstract

Low affinity immunoglobulin gamma Fc region receptor III-A (FcγRIIIa) is a cell surface protein that belongs to a family of Fc receptors that facilitate the protective function of the immune system against pathogens. However, the role of FcγRIIIa in prostate cancer (PCa) progression remained unknown. In this study, we found that FcγRIIIa expression was present in PCa cells and its level was significantly higher in metastatic lesions than in primary tumors from the PCa cohort (p=0.006). PCa patients with an elevated level of FcγRIIIa expression had poorer biochemical recurrence (BCR)-free survival compared with those with lower FcγRIIIa expression, suggesting that FcγRIIIa is of clinical importance in PCa. We demonstrated that overexpression of FcγRIIIa increased the proliferative ability of PCa cell line C4-2 cells, which was accompanied by the upregulation of androgen receptor (AR) and phosphatidylinositol-4-phosphate 5-kinase alpha (PIP5Kα), which are the key players in controlling PCa progression. Conversely, targeted inhibition of FcγRIIIa via siRNA-mediated knockdown or using its inhibitory antibody suppressed growth of xenograft PC-3 and PC-3M prostate tumors and reduced distant metastasis in xenograft mouse models. We further showed that elevated expression of AR enhanced FcγRIIIa expression, whereas inhibition of AR activity using enzalutamide led to a significant downregulation of FcγRIIIa protein expression. Similarly, inhibition of PIP5K1α decreased FcγRIIIa expression in PCa cells. FcγRIIIa physically interacted with PIP5K1α and AR via formation of protein–protein complexes, suggesting that FcγRIIIa is functionally associated with AR and PIP5K1α in PCa cells. Our study identified FcγRIIIa as an important factor in promoting PCa growth and invasion. Further, the elevated activation of FcγRIII and AR and PIP5K1α pathways may cooperatively promote PCa growth and invasion. Thus, FcγRIIIa may serve as a potential new target for improved treatment of metastatic and castration-resistant PCa.

Introduction

Fc receptors are a family of cell surface receptors that are commonly expressed by the cells in the immune system against pathogens [1, 2]. FcγRIIIa (CD16a) is an activating Fc receptor and is mainly expressed by mast cells, macrophages, neutrophils and NK cells [3, 4]. The activation of FcγRIIIa is in part dependent on its binding to the Fc portion of IgG1 antibody as shown in co-crystal structure of FcγRIIIa in complex with IgG [1].

The increased FcγRIIIa expression in monocytes/macrophages is associated with the increased cytokine production that may trigger the inflammatory and autoimmune disease conditions [5-11]. The spontaneously expansion of the circulating monocytes expressing FcγRIIIa was detected in patients with metastatic gastrointestinal carcinoma [12]. The expanded monocytes expressing FcγRIIIa have also been found in the peripheral circulations of patients with breast cancer [13]. The FcγRIIIa level was increased in blood serum from mice bearing xenograft tumors compared with mice without tumors, suggesting that FcγRIIIa expression may be associated with tumorigenesis [14]. Interestingly, FcγRIII expression was detected in prostate cancer (PCa) cell lines including LNCaP and PC-3 cells using flow cytometry analysis [15].

Recent advances in tumor immunology suggest that various types of tumors are able to escape from immunological attack by hijacking the key factors from immune cells. It is believed that tumor cells by expressing Fc receptor can block B cell normal function thereby allowing tumor cells to escape T cell-mediated cytotoxicity [16]. However, the expression and localization of FcγRIII in cancer cells and its role in tumorigenesis remains obscure.

Mice with deletion of FcγRIIIa allele had better survivals from the severe sepsis compared with the wild-type controls [17]. Moreover, mice lacking FcγRIIIa allele had reduced phagocytosis activity and decreased pro-inflammatory cytokine production in their blood cells in response to E. coli bacteria infection [18]. The monoclonal antibody mAb 3G8 against FcγRIIIa has shown promising effect on autoimmune diseases, as mAb 3G8 is able to induce clearance of the inflammatory immune complexes by selectively blocking FcγRIIIa binding to IgG [19, 20]. A bispecific-monoclonal antibody (2B1) was produced to against both c-erbR-2 onco-protein and FcγRIII protein, and 2B1 treatment suppressed growth of SK-OV-3 human ovarian tumors in xenograft mice without obvious toxicity [21]. These findings provide evidence, not only supporting a role of FcγRIIIa in autoimmune diseases, but also in tumorigenesis.

The previous reported studies have suggest that FcγRIIIa may be functionally linked to the lipid kinase phosphatidylinositol 4-phosphate 5-kinase alpha (PIP5K1α) and phosphatidylinositol 4,5-P_2(PIP2) [3, 22-24]. In the inflammatory cells, FcγRIIIa can induce cytokine production by activating downstream PI3K/AKT pathways [25-27]. We have previously shown that PIP5K1α is

a key regulator that triggers the constitutive activation of PI3K/AKT pathways in PCa cells during tumor growth and invasion [28, 29]. Conversely, the PIP5K1α inhibitor termed ISA-2011B had significantly inhibitory effect on invasive PCa in xenograft mouse models [28, 30-32]. However, it remains largely unknown whether PIP5K1α and FcγRIIIa are functionally associated in PCa cells.

In this study, we reported our novel findings on the identification of FcγRIII expression in primary cancer and metastatic tissues from PCa patient cohorts and in various subtypes of PCa cell lines. We demonstrated that FcγRIII is functionally associated with PIP5K1a/AKT and AR pathways and promoted tumor growth and invasion. We further shown that targeted inhibition of FcγRIIIa via si-RNA mediated knockdown or using inhibitory antibody suppressed growth of primary prostate tumors and reduced distant metastasis in xenograft mouse models. Our findings provide important information on new targets and options for combinational-targeted therapies for treatment of metastatic PCa.

Materials and Methods

Tissue Specimens, Tissue Microarrays, cDNA Microarrays, and CGH Arrays.

Tissue microarrays (TMAs) containing benign prostatic hyperplasia (BPH) (n=48) *vs*. matched PCa tissues (n=48) from a patient cohort (n=48 patients), and primary PCa (n=14) and metastatic PCa lesions in different organs including lymph node, liver, lung and bone/bone marrow (n=43) from 14 PCa patients were constructed at Skåne University Hospital, Malmö. The mRNA expression and copy number alteration data was extracted from the two cohorts of MSKCC datasets (n=181 primary; n=37 metastatic prostate cancer samples) [35-38], the SU2C/PCF metastatic patient cohort (n=429 cases) [33], and the TCGA cohort (n=333 cases) [34] from the Prostate Oncogenenome Project dataset in cBioPortal databases [35-38]. This study was approved by the Ethics Committee, Lund University and Umeå University. The General Data Protection Regulation (GDPR) was applied and written informed consent was obtained when required. The Helsinki Declaration of Human Rights was strictly observed.

Immunohistochemical Analysis

Immunohistochemistry on tumor tissue microarrays was performed as previously described [39]. The staining procedure was performed using a semiautomatic staining machine (Ventana ES; Ventana Inc.). The staining intensity was scored as 0 (negative), 1 (weakly positive or positive), 2

(moderate positive), or 3 (strongly or very strongly positive). The specimens were evaluated and scored by three different scientists; one of them a specialist in pathology. To evaluate the metastatic invasion of PCa cells in the bone/bone marrow of mice, femurs were fixed in 4% paraformaldehyde for 24 h before decalcification in formic acid and embedded in paraffin sections.

Cell Culturing and Treatments

PC-3 (RRID:CVCL_0035), U-937 (RRID:CVCL_0007), VCaP (RRID:CVCL_2235), LNCaP C4-2 (RRID:CVCL_4782), LNCaP (RRID:CVCL_0395) cell lines were purchased from American Type Culture Collection (Manassas, VA, USA). PNT1A (RRID:CVCL_2163) cell line was purchased from Sigma Aldrich (Stockholm, Sweden). An androgen-insensitive cell line, PC-3M (RRID:CVCL_9555) [40], was kindly provided by Dr. J Fidler (Department of Urology, MD Andersson Cancer Center, TX, USA). All human cell lines were purchased within the last three years or have been authenticated using STR profiling within the last three years. All experiments were performed with mycoplasma-free cells. For treatment with Dihydrotestosterone (DHT), medium containing 10% charcoal-stripped serum and 5 nM DHT or vehicle control 0.1% Dimethyl sulfoxide (DMSO, Sigma Aldrich) were used. Cells were treated with DHT for 12 hours. For treatment with enzalutamide (MDV3100) (Selleck Chemicals). For treatment with Enzalutamide, cells were treated with Enzalutamide at 10 μM for 6, 12 and 24 hours or vehicle control 0.1% DMSO. PIP5K1 alpha inhibitor: ISA-2011B, a diketopiperazine fused C-1 indol-3-yl substituted 1,2,3,4-tetrahydroisoquinoline derivative at final concentrations of 25 or 50 μM in 0.125% or 1% DMSO was used for treatment for 48 hours. For treatment with antibodies, PCa cells or tumor-spheroids were treated with purified anti-human FcγRIIIa monoclonal antibody (M3G8) or IgG1 isotype control at 500 ng/ml (Biolegend, USA).

Mouse models of PCa and PCa distant metastasis

The animal studies were approved by the Swedish Regional Ethical Animal Welfare Committee. Three sets of mouse experiments were performed. Athymic NMRI-*Foxn1*^{nu} nude mice were purchased from the Charles River Laboratories (Sulzfeld, Germany). The male mice (n=4-6, per experiment group) aged 4-6 weeks and weight 25-27 gram each were used in each experimental setting. (i) 1x10^6 PC-3M cells transfected with scrambled-siRNA control or FCGR3A-siRNA were implanted subcutaneously into left flank of each nude mouse. Growth and invasion of tumors

in xenograft mice were assessed (n=4 mice/group). (ii) For *in vivo* antibody-treatment of subcutaneous PCa tumors, $1x10^6$ PC-3 cells were injected subcutaneously into left flank of each mouse (n=4 per group). (iii). For antibody-treatment of metastatic PCa, 40 tumor-spheroids derived from $ALDH^{high}$ PC-3M cells were injected subcutaneously into left flank of each mouse (n=4 or 6 per group), two independent experiments were performed. To assess the frequency of PCa cells metastasized to the distant organs, xenograft mice were injected with HLA-ABC antibody conjugated with 680-DyLight NHS-ester (LifeTechnologies, Stockholm, Sweden) 6 hours before imaging. The *in vivo* imaging device (IVIS imaging system, PerkinElmer, USA) was used. For treatment of mice with purified anti-human FcγRIIIa (M3G8) monoclonal antibody (M3G8 leaf antibody, BioLegend, USA) at 5 mg/kg or isotype IgG1 via intraperitoneal injection were used twice a week. For quantitative analysis of tumor size, Living Image® software was used to measure metastatic areas and signal intensities. Bone/bone marrow samples were collected post-mortem and used for immuno-histochemical and immunoblot analyses. The animal experiments were under the licence numbers: A-12-16, A-13-16 and A3-19 approved by the Swedish Regional Ethical Committee. The animal welfare and guidelines were strictly followed. All experimental mice were kept in the ventilation cages under highly sterile conditions with 12-h light/dark cycles. The maximum number of mice was limited to four per cage. The diet and water for feeding the animals were highly sterile.

Plasmids, Transfection and siRNA Knockdowns

For siRNA-mediated knockdown, siRNA negative control duplex, on-target plus non-targeting control pool siRNA, siRNAs single oligoes or on-target siRNA SMART pool against FCGR3A (ThermoFisher and Dharmacon Inc.) were used. SiRNAs (50nM) were transfected into 1 x 10^5 PCa cells using Transfection Reagent TransIT-TKO® according to manufacturers' protocol (Mirus Bio LCC). After introduction of respective siRNA complexes into PCa cells, cells were then collected after 24-48 hours post-transfection. TransIT-TKO® was used according to the manufacturer's instructions. For transient transfection study to induce overexpression of FcγRIIIa, PIP5K1α or AR into PCa cells, pLX304-CD16A, pLPS-3'EGFP-PIP5K1α and pLPS-3'EGFP (PlasmID, Harvard Medical School, MA, USA) were used. AR plasmid vector: pCMV-AR and control pCMV vector were kindly provided by Prof. Yvonne Gwercman, Department of Translational Medicine, Lund University. Transient transfection was performed using

Lipofectamine® 2000/3000 transfection reagent (Life Technologies, UK), TransIT-2020 or TransIT-X2® (Mirus Bio, MIR5410, USA) by following the manufacturer's instructions.

Immunoblot and immunoprecipitation analysis

Immunoblot, and immunoprecipitation analysis were performed as described previously [40]. Briefly, protein from different subcellular fractions (cytoplasmic and nuclear) was isolated by using NE-PER™ Nuclear and Cytoplasmic Extraction Reagents according to manufacturer's protocol (ThermoFischer Scientific, Sweden). Densitometric quantification of immunoblots was performed by using the Image J Image Analysis Software (NIH, Baltimore, USA). For immunoblot analysis, antibodies against FCGR3A (CD16a) were purchased from Biosite. For immunoprecipitation analysis, antibody against PIP5K1α was used to pull down the immune-complexes, and antibody to IgG (ThermoFischer Scientific, Sweden) was used as a negative control.

ALDEFLUOR assay

Aldehyde dehydrogenases (ALDH) expression in PC-3M cells is used for define the cancer stem cell enriched population $ALDH^{high}$ *vs*. non-cancer stem cell population $ALDH^{low}$ populations. The $ALDH^{high}$ and $ALDH^{low}$ were sorted from PC-3M cells on FACS Aria (BD Biosciences) as previously described [40]. The ALDEFLUOR kit (StemCell Technologies, Vancouver, British Columbia, Canada) was used according to manufacturers' protocol.

Tumor-spheroid-formation assay

5×10^3 PC-3 cells were prepared in single cell suspensions and were seeded in 2 ml modified medium in 35 mm polyhema-coated culture dishes for 10 to 14 days. The modified medium contains DMEM F-12, 3.151 g/L Glucose, L-Glutamine, 1-2 x B27, 20-40 ng/ml EGF and 20-40 ng/ml FGFβ.

Immunofluorescence analysis

For staining with primary and secondary antibodies, alternatively, cell suspensions were fixed on slides in methanol in -20°C for 10 minutes. PCa cells were grown on glass coverslips in phenol red-free RPMI-1640 medium containing 10% FBS for 24 hours and fixed with 4% paraformaldehyde in PBS. The slides were stained with primary antibodies. Primary antibodies

including anti HLA-ABC conjugated with FITC, anti-FCGR3A (CD16a) was purchased from Biosite (Bioss MA, USA) and PIP5K1α (Protein Technologies, UK) was used. Secondary antibodies including anti-rabbit conjugated to Alexa Fluor 488 (Invitrogen, Stockholm, Sweden), anti-mouse conjugated to Alexa Fluor 546 (Invitrogen, Stockholm, Sweden), anti-rabbit conjugated to Rhodamine (Chemicon International Inc, Temecula, CA). Cells were counterstained with DAPI (4',6-Diamidino-2-Phenylindole, Dihydrochloride) (SERVA Electrophoresis GmbH, Heidelberg, Germany). The cells were examined under an Olympus AX70 microscope using NIS Elements F 2.20 software or a Zeiss Apoptome microscope (Zeiss, Germany), and the Zen 2.3 lite software (Zeiss, Germany).

RNA isolation and polymerase chain reaction

RNA was isolated using TRIzol™ reagent (Invitrogen, Carlsbad, CA). For cDNA synthesis, Maxima First Stand cDNA Synthesis kit was used (Thermo Scientific). The following primers were used: CD16a (NM_001127593.1) - forward: 5'-GAC AGT GTG ACT CTG AAG-3'; reverse: 5'-GCA CCT GTA CTC TCC AC-3'; GAPDH - forward: 5'-GGA TTT GGT CGT ATT GGG-3'; reverse: 5'-GGA AGA TGG TGA TGG GAT T-3'. The resultant PCR products were then subjected to electrophoresis and visualized using Proxima C16Phi+ bio-imaging system (Isogen Life Science). Semi-quantifications of the results were performed using ImageJ program.

Proliferation Assay

Proliferation of the cells were determined using MTS proliferation assays (Promega Biotech) according to manufacturer's protocol. Cells at 5 x 10^3 cells per well were cultured in a 96-well plates for 48 hours. MTS incorporation into the DNA was determined by measuring the absorbance at both 490 nm on an ELISA plate reader Infinite® M200 multimode microplate reader (Tecan Sunrise™).

Luciferase Assays

PC-3 cells were transiently transfected with different vectors along with the reporter vector containing luciferase gene (Luc) or full-length cyclin A1 promoter in Luc reporter vector (cyclin A1-Luc) as indicated. The Firefly Luciferase and Renilla Luciferase activity were determined by using an Infinite® M200 multimode microplate reader (Tecan Sunrise™), equipped with dual injector. For AR receptor activity assay in LNCaP cells, AR Cignal Reporter Assay Kit (Qiagen

Inc.) was used according to the manufacturers protocol. Briefly, LNCAP cells were transiently transfected with different vectors along with the reporter vector ARE-Luciferase (ARE Luc) vector as indicated. The Firefly and Renilla Luciferase with Dual Luciferase Assay Kit (Promega) according to standard protocol in the Tecan Infinite M200 (Tecan Trading AG) plate reader equipped with dual injector.

Migration assay

Cell migration assays were performed using Transparent PET Membrane chambers (Corning, Germany). A total of 0.5–2 × 10^5 cells in RPMI 1640 phenol red-free and serum-free medium were seeded in the upper chamber, and RPMI-media supplemented with 50% serum as a chemoattractant was loaded in the lower chamber to allow the migration to proceed. The migrated cells were stained after 18 hours or 24 hours and the proportion of migrated cells was calculated as described [41].

Statistical analysis

Tukey-test, *T-test,* Kruskal Wallis/ANOVA and Spearman rank correlation tests were performed. Student t-test was used for statistical analyses of the experimental data. The standard deviation (SD) is an indication of variability of all samples. The precision of the sample mean is indicated by standard error. Confidence levels are expressed using 95% confidence interval (CI). All statistical testes were two-sided, and *p* values less than 0.05 were considered to be statistically significant. Data presented is representative of at least two or three independent experiments. Distribution of overall survival (OS) or disease-free survival/biochemical recurrence-free survival (BRFS) was estimated by the method of Kaplan-Meier, with 95% confidence intervals. Differences between survival curves were calculated using the log-rank test. Statistical softwares, Social Sciences software (SPSS, version 21, Chicago), and GraphPad Software were used.

Results

Clinical relevance of FcγRIIIa expression in patients with PCa metastasis and its correlation with PIP5K1α

To investigate the role of FcγRIIIa in tumorigenesis and progression of PCa, we firstly examined FcγRIIIa expression in primary tumors and metastatic lesions from PCa patients. FcγRIIIa protein expression was assessed by using immunohistochemical analysis on the tissue microarrays

(TMAs) consisting of benign prostate hyperplasia (BPH), adjacent primary PCa and metastatic PCa lesions in lymph nodes, bone marrows and lungs from patients with primary and metastatic PCa. FcγRIIIa expression was found in the epithelium of BPH tissues (Figure 1a). Further, FcγRIIIa was expressed by the primary cancer tissues and its expression was nearly significantly higher in the primary PCa tissues as compared with that in the BPH (p=0.051, Figure 1a). We found that FcγRIIIa was highly expressed in the metastatic lesions in the bone marrows, lymph nodes and lungs from patients who suffered metastatic PCa (Figure 1a). Statistical analysis revealed that FcγRIIIa protein expression was significantly higher in metastatic lesions compared with that of primary tumors (p=0.006) (Figure 1b). We next examined FcγRIIIa mRNA expression in the MSKCC patient cohort from the Prostate Oncogenenome Project dataset in cBioPortal databases [35]. Similar to its protein expression in PCa tissues, FcγRIIIa mRNA expression was found in primary and metastatic PCa from the MSKCC cohort which contained over 95% of cancer cells in the tumor tissues. Further, expression of FcγRIIIa mRNA was significantly higher in metastatic lesions (n=19) than that of primary tumors (n=131) (p<0.01, Figure 1c). We have previously reported that PIP5K1α is a key player in PCa progression and metastasis. We therefore wanted to assess whether elevated level of FcγRIIIa expression might be associated with abnormal PIP5K1α expression in PCa primary and metastatic cancer tissues. Spearman's rank correlation test was performed, which revealed that there was a statistically significant correlation between FcγRIIIa and PIP5K1α protein expression in primary and metastatic cancer tissues from the PCa patient cohorts (R^2= 0.480, p<0.001; Table 1). In addition, FcγRIIIa expression correlated with cyclin A1 in cancer tissues from the same patient cohorts (p=0.001; Table 1). To further assess the clinical importance of FcγRIIIa expression, we examined the association between FcγRIIIa expression and biochemical recurrence (BCR)-free survival of the patients using Kaplan-Meier survival analysis. We found that PCa patients with higher FcγRIIIa mRNA expression in their tumors (n=12) had worse biochemical recurrence (BCR)-free survival compared to those with lower FcγRIIIa expression (n=127) (p=0.026) (Figure 1d). Next, we wanted to assess whether alterations in *FCGR3A* gene encodes for FcγRIIIa might be a frequent event in metastatic PCa. To this end, we examined genomic alterations in *FCGR3A* along with *AR, PIP5K1A and PTEN* using a large SU2C/PCF metastatic PCa cohort (n=429) [33]. We found that *FCGR3A* gene amplifications and mRNA upregulation account for 9% of the metastatic PCa cases. Interestingly, 61% cases of this cohort had AR gene amplifications and mRNA upregulation, and 19% had *PIP5K1A* gene amplification and mRNA upregulation. Conversely, *PTEN* gene mutation, deletion

or mRNA downregulation accounted for 37% of this metastatic PCa cohort (Figure 1e). This data indicates that *FCGR3A* amplification and mRNA upregulation is likely associated with PCa metastatic status. To further assess the clinical importance of FcγRIIIa mRNA expression in PCa progression, we examined FcγRIIIa mRNA expression in primary tumors from the TCGA PCa cohort, which were divided into four subgroups based on the Gleason grade scores (n=333 cases) [34]. FcγRIIIa mRNA expression was significantly higher in the primary tumors with Gleason scores higher than 8 compared with those with lower Gleason grades (3+3 or 3+4) (p<0.01) (Figure 1f). This data showed that FcγRIIIa mRNA expression was elevated in the advanced PCa, suggesting the clinical importance of FcγRIIIa expression in PCa. Gene alterations in the *FCGR3A* loci were found in 6% of this PCa cohort, which was similar to what was observed for AR (Figure 1g). In the MSKCC/DFCI patient cohort consisting primary PCa (n=1013 PCa cases) from the Prostate Oncogenenome Project dataset in cBioPortal databases [42], *FCGR3A* gene alterations were found in 3% of PCa cases, which was similar to *PIP5K1A* gene alterations accounted for 5% in this PCa cohort (Supplemental Figure 1). No statistically significant correlations between AR and FcγRIIIa mRNA expression were found in SU2C/PCF metastatic PCa cohort and TCGA cohort (Supplemental Figure 2 and 3).

FcγRIIIa expression in PCa cells is involved in tumor growth

To validate the presence of FcγRIIIa expression in PCa cells, we used castration-resistant PCa cell line, PC-3 cells to examine the FcγRIIIa mRNA expression. Since cancer cells utilize inflammatory myeloid cells to stimulate growth signaling in cancer cell, we co-cultured PC-3 cells with monocytes U-937 cells to examine the expression of FcγRIIIa in PC-3 cells after being co-cultured with U-937 cells. FcγRIIIa mRNA expression was observed in PC-3 cells and U-937 cells cultured alone as well as in PC-3 cells from the co-culture with U-937 cells as determined by the semi-quantitative RT-PCR analysis using the primers specific for *FCGR3A* gene (Supplemental Figure 4a). The sequence of the PCR product of *FCGR3A* from PC-3 cells exhibited 100% match with the consensus sequence of *FCGR3A* from NCBI database (Supplemental Figure 4b). Next, we examined FcγRIIIa protein expression in PC-3 cells along with various types of PCa cell lines by using immunoblot analysis. Interestingly, FcγRIIIa protein exhibited high level in the castration-resistant cell lines including C4-2, VCaP, PC-3 and PC-3M cells, while its expression level appeared to be relatively low in the non-malignant PNT1A cells (Supplemental Figure 5).

Since FcγRIIIa expression is significantly elevated in metastatic PCa tissues compared with the primary PCa tumors, we wanted to elucidate the role of FcγRIIIa in PCa progression. To this end, we transfected C4-2 cells with a full-length FcγRIIIa expressing plasmid or a control vector to induce FcγRIIIa overexpression. Overexpression of FcγRIIIa was confirmed by immunoblot analysis (Figure 2a). To examine the effect of FcγRIIIa overexpression on tumor growth, we subjected C4-2 cells that expressed FcγRIIIa or control vector to the 3-D tumor spheroid assays. We found that C4-2 cells overexpressing FcγRIIIa gave rise to higher numbers of tumor-spheroids than that of controls (p=0.0057, Figure 2b). This suggests that elevated level of FcγRIIIa in PCa cells led to increased ability of tumorigenesis of PCa cells *in vitro*. Since steroid hormone DHT promotes growth of PCa by inducing activation of AR pathways that are associated with PCa growth and invasion, we therefore examined the relationship between DHT/AR pathways and FcγRIIIa expression in PCa cells. We employed C4-2 cell line to DHT treatment, and examined the effect of DHT on FcγRIIIa expression. We found that DHT treatment at 5 nM resulted in increased FcγRIIIa expression, which was equivalent to its effect on induction of AR expression in C4-2 cells (Figure 2c). Thus, FcγRIIIa expression is responsive to androgen stimulation in PCa cells. As mentioned above, we found a significant correlation between FcγRIIIa and PIP5K1α in primary tumor and metastatic lesions from PCa patients. Given that PIP5K1α acts on upstream of AR pathways, we next investigated the relationship between FcγRIIIa and AR, as well as the interaction between FcRIIIa and PIP5K1. Induced overexpression of FcγRIIIa led to a slight increase in AR and PIP5K1α in C4-2 cells compared with the controls. However, the statistically significance was not achieved (Figure 2d and e). Next, we examined the effect of FcγRIIIa depletion on expression of AR and PIP5K1α in C4-2 cells. FcγRIIIa was silenced via siRNA-mediated knockdown in C4-2 cells. The significant down-regulation of FcγRIIIa in C4-2 cells compared with that of si-RNA control was confirmed using immunoblot analysis (p=0.024, Figure 2f and g). We found that silence of FcγRIIIa led to the down-regulation of PIP5K1α and AR expression as compared with that of siRNA controls in C4-2 cells (for PIP5K1α, p=0.005; for AR, p=0.001; Figure 2f and g). Thus, FcγRIIIa depletion has significant effect on the expression of PIP5K1α and AR, suggesting that FcγRIIIa is required by PCa cells to regulate PIP5K1α and AR expression.

To further determine the relationship among FcγRIIIa, AR and PIP5K1α in PCa cells, we performed immunoprecipitation assays to examine whether FcγRIIIa may form protein-protein complexes with AR and PIP5K1α in C4-2 cells. We found that both FcγRIIIa and AR were

present in the immuno-complexes that are associated with PIP5K1α (Figure 2h). This suggests that FcγRIIIa is able to form protein complexes with PIP5K1α and AR as well. Thus, FcγRIIIa is functionally linked to AR and PIP5K1α via protein-protein interaction. Immunofluorescent analysis was performed to examine the subcellular localization of FcγRIIIa in C4-2 cells. We found that FcγRIIIa expression was highly enriched in the membrane/cytoplasmic compartments, and appeared to be co-localized with PIP5K1α in the membrane compartment of C4-2 cells (Figure 2i).

The functional association between AR and FcγRIIIa in PCa cells

To gain deeper understanding of the mechanisms underlying the association between FcγRIIIa and AR in PCa cells, we examined the effect of AR overexpression on FcγRIIIa expression at protein and mRNA levels. AR overexpression was induced in LNCaP cells by transfecting the cells with a vector carrying full-length AR or a control vector. We found that elevated expression of AR resulted in a significant increase in FcγRIIIa protein expression in LNCaP cells as compared with that of control (p= 0.03, Figure 3a). However, AR overexpression had no significant effect on FcγRIIIa mRNA expression in LNCaP cells, as determined by using semi-quantitative RT-PCR analysis (Supplemental Figure 6). Since Enzalutamide is an inhibitor for AR and it targets ligand-binding domain of AR, resulting in inhibition of AR activity. We therefore examined whether inhibition of AR using enzalutamide might have a direct effect on FcγRIIIa protein and mRNA expression. To this end, we treated LNCaP cells with enzalutamide for 6 hours, 12 hours and 24 hours respectively. We then examined the effect of AR inhibition by enzalutamide on the expression of AR, FcγRIIIa, and PSA, a known downstream target of AR. As expected, enzalutamide treatment resulted in significant decrease in AR expression after 6 hours of treatment and throughout 12 to 24 hours (for AR, enzalutamide treatment vs. control treatment for 6 hours, p=0.026; 12 hours, p=0.003 and 24 hours, p=0.021; Figure 3b, c and d). Interestingly, enzalutamide treatment led to a significant down-regulation of FcγRIIIa protein expression readily after 12 hours and throughout 24 hours of post-treatment (enzalutamide treatment *vs.* control treatment for 6 hours, p=0.325, for 12 hours, p=0.03 and for 24 hours, p=0.034, Figure 3b, c and d). Enzalutamide did not appear to have significant effect on FcγRIIIa mRNA expression in LNCaP cells as measured by quantitative RT-PCR (Supplemental Figure 7). The effect of AR-inhibition on FcγRIIIa readily appeared at early time point of 12 hours, and LNCaP is a slow

proliferating PCa cell line with a doubling time at approximately 60 hours, these findings suggest that AR and FcγRIIIa may be directly under each other's control.

The role of FcγRIIIa in AR-independent castration-resistant PC-3 cells

To further elucidate the role of FcγRIIIa and the underlying cellular mechanisms in PCa growth and progression, we employed PC-3 cells that lack functional AR, which represent an ideal model to assess the relationship between FcγRIIIa and PIP5K1α. To do this, FcγRIIIa over-expression was induced in PC-3 cells by transfecting the cells with a vector carrying full-length FcγRIIIa or a control vector, and FcγRIIIa overexpression was verified by immunoblot analysis (Figure 4a). We found that elevated expression of FcγRIIIa resulted in a significant increase in PIP5K1α expression as compared with the control (p= 0.02, Figure 4a). The effect of FcγRIIIa overexpression on growth of PC-3 tumor was determined using tumor-spheroid assays. Similar to what was observed in C4-2 cells, FcγRIIIa overexpression resulted in increased ability of PC-3 cells to form tumor-spheroids as compared with the controls (p=0.001, Figure 4b). This data suggest that FcγRIIIa overexpression is able to promote tumorigenesis in PC-3 cell model.

To elucidate the role of FcγRIIIa in PCa progression, we assessed the effect of FcγRIIIa overexpression on migratory ability of PC-3 cells. PC-3 cells that overexpressed FcγRIIIa displayed significantly higher migratory ability compared with the control (p< 0.001 Figure 4c).

To further assess the functional importance of FcγRIIIa in tumor progression, we silenced FcγRIIIa using siRNA-mediated knockdown. PC-3 cells that were transfected with siRNA to FcγRIIIa or control siRNA were subjected to the tumor-spheroid formation assays. In contrast to the effect of FcγRIIIa overexpression on tumor-spheroid formation, silence of FcγRIIIa led to remarkable decrease in ability of PC-3 cells to form tumor-spheroids relative to that of controls (p=0.012, Figure 4d and e). This suggests that elevated level of FcγRIIIa is functional important for PCa cells to gain tumorigenic ability. Similar to what was observed in C4-2 cells, siRNA-mediated knockdown of FcγRIIIa led to a significant down-regulation of PIP5K1α expression (p=0.011, Figure 4f). Next, we examined the effect of inhibition of PIP5K1α on FcγRIIIa in PC-3 cells. We applied a selective inhibitor of PIP5K1α, ISA-2011B and examined ISA-2011B on FcγRIIIa in PC-3 cells. Interestingly, inhibition of PIP5K1α by ISA-2011B resulted in decreased FcγRIIIa expression, which was coincident with the down-regulation of pAKT induced by ISA-2011B in PC-3 cells as compared with controls (Figure 4g). Similar to what was shown in Figure

3, this data also shows that PIP5K1α and FcγRIIIa mutually affect each other, which further support our observation on that PIP5K1α and FcγRIIIa form protein-protein complexes, as mentioned in Figure 2. PIP5K1α promotes prostate cancer cell survival and invasion through regulation of expression of AR in PCa cells [28, 29]. To this end, we wanted to investigate whether FcγRIIIa and PIP5K1α might act as co-regulators of AR to enhance transcriptional activity of AR on its target genes, we utilized a cyclin A1 full-length promoter-luciferase reporter construct as described [43], and examined the effect of FcγRIIIa and PIP5K1α on AR transcriptional activity on its target gene cyclin A1 in PC-3 cells. AR alone increased remarkably cyclin A1-luciferase activity as compared with that of controls (p=0.003, Figure 4h). FcγRIIIa had no additive effect on AR to further enhance cyclin A1-promoter activation (Figure 4h). Interestingly, PIP5K1α and AR in combination increased remarkably cyclin A1-luciferase activity as compared to that of AR alone (p=0.008, Figure 4h). These data suggest that FcγRIIIa may serve as a co-regulator of AR via PIP5K1α. To further elucidate the functional impact of FcγRIIIa on the downstream target genes in PCa cells, we employed androgen-dependent LNCaP cells and carried out dual-luciferase assays by using androgen responsive (ARE) luciferase reporter construct. FcγRIIIa overexpression induced ARE reporter luciferase activity, which led to an increase in ARE promoter activity by 100% relative to controls in LNCaP cells (p=0.013, Figure 4i). Thus, FcγRIIIa is able to mediate the transcriptional activity of the key factors that contribute to PCa progression.

Targeted inhibition of FcγRIIIa in PC3M cells reduced tumor growth in xenograft mice

We have previously reported that PC-3M cells are able to initiate metastasis to distant organs in xenograft mice [40]. We therefore employed PC3M xenograft tumor models in mice to elucidate the role of FcγRIIIa in PCa progression. To this end, we silenced FcγRIIIa in PC3M cells by using si-RNA mediated knockdown. We then implanted subcutaneously equal amount of si-FcγRIIIa PC-3M cells and si-control PC-3M cells into the nude mice. The growth of PC-3M tumors in xenograft mice were measured and monitored. At the end of experiments, the mean tumor volumes in mice that received si-FcγRIIIa PC-3M cells were significantly smaller than that of controls (p=0.020, Figure 5a). We then assessed expression of the key marker proteins including Ki-67, phosphorylated AKT, MMP9 and VEGFR2 that control proliferation and invasiveness of PCa cells. Consistent with what was observed on the tumor volumes, si-FcγRIIIa PC-3M tumors displayed a significantly reduced proliferation rate relative to controls, as determined by using Ki-

67 staining (p<0.001, Figure 5b). Similarly, we found that expression of PIP5K1α, pSer-473AKT, MMP9 and VEGFR2 was significantly down-regulated in si-FcγRIIIa PC-3M tumors compared with that of si-control tumors, which was coincident with the reduced volumes of si-FcγRIIIa PC-3M tumors (for PIP5K1α expression, p=0.048; for pAKT, p=0.0045; for MMP9 expression, p=0.028 and for VEGFR2, p<0.001; Figure 5c, d, e and f). We have previously reported that PC-3M cells are able to initiate metastasis to distant organs in xenograft mice [40]. We therefore examined the apparent metastasis in the lymph nodes in mice that have received si-FcγRIIIa PC-3M or si-control PC3M cells. We found that mice bearing si-control PC-3M tumors had lymph node metastasis, whereas mice bearing si-FcγRIIIa tumors were free of lymph node metastasis (Figure 5g). Further, si-control PC-3M tumors expressed cytokeratin 19 (CK19) and vimentin, the human epithelial cell markers. In contrast, si-FcγRIIIa tumors were negative to CK19 and vimentin expression. This data suggests that inhibition of FcγRIIIa greatly reduced growth and metastatic potentials of primary tumors in xenograft mouse models. It is likely that FcγRIIIa promotes PCa growth and invasion via its down-stream PIP5K1α/AKT and VEGFR2 signaling pathways.

Inhibitory effect of anti-FcγRIIIa antibody on PCa growth in PCa cell line models and in PCa xenograft mice

To further study the role and cellular mechanisms of FcγRIIIa in tumor growth and invasion, we examined the anti-tumor effect of anti-FcγRIII antibody (M3G8) in *in vitro* and *in vivo* systems. We subjected PC-3 cells to the formation of tumor-spheroids. The tumor-spheroids were then subjected to the treatment with M3G8 or control antibody. We observed that M3G8-treatment led to a remarkably reduced number of tumor-spheroids as compared with controls (p=0.028, Figure 6a). Also, there was a pronounced alteration in cell-cell contacts and a reduced phalloidin-staining in tumor-spheroids treated with M3G8 compared with that of controls (Figure 6b).

Next, we wanted to investigate whether blockade of FcγRIIIa using purified anti-human FcγRIII monoclonal antibody termed M3G8 may suppress growth of PCa tumors in xenograft mice. To this end, we established xenograft mice bearing subcutaneously implanted PC-3 tumors, which were less invasive, but grow rapidly as compared to PC-3M tumors. PC-3 tumors were allowed to grow into approximately 300 mm^3 in size, and were randomized into two groups. The two groups of mice were treated with M3G8 or control antibody. The M3G8-treated group had tumors which

were 4-fold smaller in size relative to the control group after treatment for 21 days (mean volume of tumors in control group and M3G8 group were 1612 mm^3 and 436 mm^3, respectively, difference =1176 mm^3; 95% CI=384-486, $p<0.01$, Figure 6c). This was consistent with the inhibitory effect of targeted inhibition of FcγRIIIa on PC-3M tumors shown above. Immunohistochemical analysis of tumor tissues further revealed that M3G8-treated tumors exhibited reduced expression of PIP5K1α and VEGFR2 as compared to that of controls (for PIP5K1α, $p = 0.01$; for pAKT, $p = 0.02$ and for VEGFR2, $p = 0.01$, figure 6d and e).

Inhibitory effect of anti-FcγRIIIa antibody on PCa growth and metastasis in mice

Next, we wanted to investigate whether blockade of FcγRIIIa using M3G8 may reduce/inhibit distant metastasis of PCa. We have previously reported that $ALDH^{high}$ stem-like sub-populations isolated from PC-3M cells initiated metastatic growth in distant organs such as bone/bone marrow in xenograft mice [40]. To this end, we sorted stem-like $ALDH^{high}$ subpopulations of PC3M cells using FACS-based ALDEFLUOR assay and subjected the stem-like $ALDH^{high}$ subpopulations to the formation of 3-dimensional tumor-spheroid (Figure 7a). The tumor-spheroids were then implanted subcutaneously into the nude mice (40 tumor-spheroids/mouse) to allow formation of distant metastasis (Figure 7a). Virtually all mice that received tumor-spheroids had developed distant metastasis 60 days post-implantation, as measured and quantified by using *in vivo* imaging assays as described previously [40] (Figure 7b and c). Mice bearing metastatic lesions were randomized into two groups and were treated with intraperitoneal injection of M3G8 or control antibody at 5 mg/kg dose (Figure 7b and c). At the end of the experiments, there was a significant reduction in metastatic burdens in mice treated with M3G8 compared with that of control, as quantified using *in vivo* imaging analysis (p=0.039, Figure 7b and c). M3G8 treatment did not induce weight-loss or other detectable adverse events in the mice. There was a significant higher proportion of cells positive to Cytokeratin 19 (CK19), a marker of human epithelial cell origin, in the bone marrows from xenograft mice treated with control antibody compared with those treated with M3G8 (p=0.02, figure 7d). These data suggest that inhibition of FcγRIIIa inhibits metastatic growth of PCa cells in distant organs in xenograft mice.

To test the therapeutic potentials of combination therapies of M3G8 and ISA-2011B, we assessed the effects of M3G8, ISA-2011B alone or in combination on the invasiveness of C4-2 cells. C4-2 cells that were treated with M3G8 or ISA-2011B alone or in combination were subjected to the

migration assays. Similar to ISA-2011B, M3G8 treatment alone significantly reduced migratory ability of C4-2 cells (for M3G8, *p=0.016*; for ISA-2011B, *p=0.006*, Figure 7e). Combination of M3G8 and ISA-2011B had greater inhibitory effect as compared to that of M3G8 alone on the migratory ability of C4-2 cells (for combination of M3G8 and ISA-2011B vs. control, p=0.003; for combination of M3G8 and ISA-2011B vs. M3G8, p=0.011, Figure 7e). These data suggest that combination treatment using M3G8 and ISA-2011B may have an additive inhibitory effect on PCa cells.

Discussion

In this study, we discovered that the expression of FcγRIIIa was significantly higher in metastatic lesions than that of primary cancer tissues. Moreover, high level of FcγRIIIa was significantly associated with poor prognosis in PCa patients. We for the first time showed that FcγRIIIa was expressed in PCa cells from primary tumor tissues and metastatic lesions and PCa cell lines as well. FcγRIIIa expression was significantly higher in metastatic lesion compared to that of primary tumor tissues. We showed that *FCGR3A* gene amplifications and mRNA upregulation accounted for 9% of the metastatic PCa cases, in which 61% cases had AR gene amplifications and mRNA upregulation, 19% had *PIP5K1A* gene amplification and mRNA upregulation, and 37% cases had *PTEN* gene mutation, deletion or mRNA downregulation. Furthermore, PCa patients with higher FcγRIIIa mRNA expression in their tumors had worse biochemical recurrence (BCR)-free survival compared to those with lower FcγRIIIa expression. Our data suggests that FcγRIIIa expression is highly clinical relevant and may reflect its role in PCa development and progression.

In this study, we aimed to investigate whether FcγRIIIa may play an important role in growth and invasion of PCa at both AR-dependent and AR-independent fashions. We found that induced overexpression of FcγRIIIa in C4-2 cells promoted cancer cell growth. Conversely, inhibition of FcγRIIIa via si-RNA-mediated knockdown reduced growth ability of C4-2 cells. Similarly, induced overexpression of FcγRIIIa led to increased expression of AR and PIP5Kα, the key factors that promote PCa growth and invasion, while inhibition of FcγRIIIa led to decreased expression of AR and PIP5K1α.

One of the striking findings in this study is the identification of the underlying mechanism by which FcγRIIIa and AR interact with each other in PCa cells. We found that FcγRIIIa was

capable of inducing AR target gene promoter activation as determined by using the ARE reporter luciferase activity assays. Furthermore, overexpression of AR led to significant increase in FcγRIIIa protein expression, while inhibition of AR by using enzalutamide decreased FcγRIIIa protein expression readily after 12 hours of enzalutamide treatment of LNaP cells. In addition, we showed that AR and FcγRIIIa interacted with each other through formation of protein-protein complexes together with PIP5K1α. Our findings suggest that the observed effect of FcγRIIIa on AR may not be the consequence of FcγRIIIa-induced cell proliferation in AR-expressing PCa cells, but rather due to that FcγRIIIa is functionally associated with AR and PIP5K1α associated pathways via protein-protein interactions.

Interestingly, induced overexpression of FcγRIIIa in androgen-independent PC-3 cells that do not express functional AR also promoted proliferation and invasion of PC-3 cells. Conversely, inhibition of FcγRIIIa using si-RNA mediated knockdown led to significant decrease in growth and invasion of PC-3 cells *in vitro* and PC-3 tumors in xenograft mice. Although the underlying mechanisms by which FcγRIIIa promotes PCa growth and invasion at AR-independent fashion remain obscure, our findings in *in vitro* and *in vivo* model systems provide strong evidence suggesting that FcγRIIIa plays an important role in AR-independent fashion. It has been reported that activation and expression of FcγRIIIa in immune cells are associated with the formation of immune complexes, and increased FcγRIIIa expression can lead to the subsequent activation of PI3K/AKT pathways in immune cells [1]. It is known that FcγRIIIa is activated by IgG immune complexes. Thus, the interaction between FcγRIIIa and IgG immune complexes is critical for FcγRIIIa internalization to enable the activation of FcγRIIIa downstream signaling events related to migration and survival of leukocytes [2]. It will be of great interests to investigate whether FcγRIIIa may utilize the IgG immune complexes from the PCa-associated immune cells/tumor microenvironment to promote growth and progression of castration-resistant PCa.

Our results further showed that PIP5K1α was functionally associated with FcγRIIIa, as inhibition of both PIP5K1α and FcγRIIIa resulted in greater inhibition of invasiveness of PCa cells as compared with inhibition of FcγRIIIa alone. Further, these key molecules organize and activate several signaling pathways, leading to tumor cell survival and invasion. We plan to further investigate the role of FcγRIII and the underlying mechanisms in PCa progression from androgen-dependence to castration-resistant state in the near future.

In this study, we applied xenograft models Targeted inhibition of FcγRIIIa via siRNA-mediated knockdown or using inhibitory antibody suppressed growth of primary prostate tumors and reduced distant metastasis in xenograft mouse models. We further established novel metastatic xenograft mouse models to examine the effect of inhibition of FcγRIIIa activity on PCa metastasis. Further, our findings suggest that FcγRIIIa plays an important role in PCa progression and is a potential therapeutic target for the development of the new treatment strategies for advanced and metastatic PCa. Since elevated activity of FcγRIIIa can be inhibited using blockade antibody M3G8, we therefore examined the effect of M3G8 on PCa tumor growth and metastasis. Our data showed that M3G8 significantly suppressed tumor growth *in vitro* and in xenograft mouse models. M3G8 blocks both FcγRIIIa and FcγRIIIb, we found that M3G8 treatment led to an inhibition of FcγRIIIa and reduced expression of PIP5K1α/AKT, as determined by our immunoblot analysis by using antibody against FcγRIIIa, Further, the inhibitory effect of M3G8 treatment on PCa tumor growth is comparable to the effect of FcγRIIIa knockdown on PCa tumor growth.

Several previous studies have demonstrated that FcγRIIIa is a signal molecule that induces rapid and transient PIP5K1α membrane recruitment on NK cells to facilitate cytotoxic killing [44]. It is likely that PCa cells utilize FcγRIIIa to mimic immune cells and to evade cytotoxic cell-mediated antitumor immunity.

Conclusions

Our results showed that treatment approach by optimizing activity to blocking antibody to FcγRIIIa, is likely the good strategy to improve the therapeutic outcome by using antibody-mediated destruction of malignant cells. Taken together, our findings suggest that FcγRIIIa may serve as a potential new target for improvement of treatment of metastatic and castration-resistant PCa.

Acknowledgements

This work was supported by grants from the Swedish Cancer Society (CAN-2017-381), The Swedish Children Foundation (TJ2015-0097), H2020-MSCA-ITN-2018-European Commission

(721297), The Swedish National Research Council (2019-01318), STINT Institutional Grant (IG2013-5595), Malmö Cancer Foundation, the Government Health Innovation Grant, Medical Faculty, Lund University, Kempe STF, Umeå University, Medical Faculty Grants, Norland fund for Cancer Forskning, Insamlings Stiftelsen, Umeå University, Bioteknik medel, Medical Faculty, Umeå University and Medical Faculty infrastructure Grants, Umeå University to JLP. The Grant from UCMR to JLP and SNW. The Grants from University of Copenhagen to NØ. The Royal Physiographical Foundation to MS. We sincerely thank Yvonne Lundberg Giwercman (Lund University, Lund) for providing reagents for this study. We thank the facilities and technical assistance of Niki Choo of the Umeå Core Facility for Electron Microscopy (UCEM) at the Chemical Biological Centre (KBC), Umeå University.

Conflict of Interest

No Conflict of Interest exists for this manuscript.

Author Contributions

RK, PFL, MS, RM, NØ and JLP designed experiments. RK, PFL, MS, RM, TW, ASSK, AH, AA, SC, JS, AK, AS and KEH performed experiments. RK, PFL, MS, RM, TW, ASSK, AH, AJ, SC, JS, AA, AS, NPM, DH, TG, BR and JLP performed data analysis. RK, PFL, MS, TW, ASSK, NPM, DMH, SNW, DÖ, TG, NØ and JLP and JLP contributed to major manuscript writing. All authors contributed to final editing and final approval of the manuscript.

Data accessibility

All data analyzed for this study are included in this published article and its supplemental information files. The data will be made available from the corresponding authors upon reasonable request.

References

1. Nimmerjahn F & Ravetch JV (2008) Fcγ receptors as regulators of immune responses. *Nature Reviews Immunology* 8, 34-47.

2. Bournazos S, Gupta A & Ravetch JV (2020) The role of IgG Fc receptors in antibody-dependent enhancement. *Nature Reviews Immunology* 20, 633-643.

3. Baniyash M (2004) TCR zeta-chain downregulation: curtailing an excessive inflammatory immune response. *Nat Rev Immunol* 4, 675-687.

4. Baudino L, Nimmerjahn F, Azeredo da Silveira S, Martinez-Soria E, Saito T, Carroll M, Ravetch JV, Verbeek JS & Izui S (2008) Differential contribution of three activating IgG Fc receptors (FcgammaRI, FcgammaRIII, and FcgammaRIV) to IgG2a- and IgG2b-induced autoimmune hemolytic anemia in mice. *J Immunol* 180, 1948-1953.

5. Abrahams VM, Cambridge G, Lydyard PM & Edwards JC (2000) Induction of tumor necrosis factor alpha production by adhered human monocytes: a key role for Fcgamma receptor type IIIa in rheumatoid arthritis. *Arthritis Rheum* 43, 608-616.

6. Edwards JC & Cambridge G (1998) Rheumatoid arthritis: the predictable effect of small immune complexes in which antibody is also antigen. *Br J Rheumatol* 37, 126-130.

7. Kramer PR, Kramer SF & Guan G (2004) 17 beta-estradiol regulates cytokine release through modulation of CD16 expression in monocytes and monocyte-derived macrophages. *Arthritis Rheum* 50, 1967-1975.

8. Pettipher ER, Higgs GA & Henderson B (1986) Interleukin 1 induces leukocyte infiltration and cartilage proteoglycan degradation in the synovial joint. *Proc Natl Acad Sci U S A* 83, 8749-8753.

9. Pettipher ER, Higgs GA & Henderson B (1986) Arthritogenic activity of interleukin 1. *Agents Actions* 19, 337-338.

10. Saklatvala J (1986) Tumour necrosis factor alpha stimulates resorption and inhibits synthesis of proteoglycan in cartilage. *Nature* 322, 547-549.

11. Wooley PH, Dutcher J, Widmer MB & Gillis S (1993) Influence of a recombinant human soluble tumor necrosis factor receptor FC fusion protein on type II collagen-induced arthritis in mice. *J Immunol* 151, 6602-6607.

12. Saleh MN, Goldman SJ, LoBuglio AF, Beall AC, Sabio H, McCord MC, Minasian L, Alpaugh RK, Weiner LM & Munn DH (1995) CD16+ monocytes in patients with cancer: spontaneous elevation and pharmacologic induction by recombinant human macrophage colony-stimulating factor. *Blood* 85, 2910-2917.

13. Feng AL, Zhu JK, Sun JT, Yang MX, Neckenig MR, Wang XW, Shao QQ, Song BF, Yang QF, Kong BH & Qu X (2011) CD16+ monocytes in breast cancer patients: expanded by monocyte chemoattractant protein-1 and may be useful for early diagnosis. *Clin Exp Immunol* 164, 57-65.

14. Lynch A, Tartour E, Teillaud JL, Asselain B, Fridman WH & Sautes C (1992) Increased levels of soluble low-affinity Fc gamma receptors (IgG-binding factors) in the sera of tumour-bearing mice. *Clin Exp Immunol* 87, 208-214.

15. Liu AY (2000) Differential expression of cell surface molecules in prostate cancer cells. *Cancer Res* 60, 3429-3434.

16. Nelson MB, Nyhus JK, Oravecz-Wilson KI & Barbera-Guillem E (2001) Tumor Cells Express FcγRl Which Contributes to Tumor Cell Growth and a Metastatic Phenotype. *Neoplasia* 3, 115-124.

17. Zhang D, He J, Shen M & Wang R (2014) CD16 inhibition increases host survival in a murine model of severe sepsis. *J Surg Res* 187, 605-609.

18. Bloemendaal FM, Levin AD, Wildenberg ME, Koelink PJ, McRae BL, Salfeld J, Lum J, van der Neut Kolfschoten M, Claassens JW, Visser R, Bentlage A, D'Haens G, Verbeek JS, Vidarsson G & van den Brink GR (2017) Anti-Tumor Necrosis Factor With a Glyco-Engineered Fc-Region Has Increased Efficacy in Mice With Colitis. *Gastroenterology* 153, 1351-1362 e1354.

19. Yu X, Menard M, Prechl J, Bhakta V, Sheffield WP & Lazarus AH (2016) Monovalent Fc receptor blockade by an anti-Fcgamma receptor/albumin fusion protein ameliorates murine ITP with abrogated toxicity. *Blood* 127, 132-138.

20. Hogarth PM & Pietersz GA (2012) Fc receptor-targeted therapies for the treatment of inflammation, cancer and beyond. *Nat Rev Drug Discov* 11, 311-331.

21. Weiner LM, Holmes M, Adams GP, LaCreta F, Watts P & Garcia de Palazzo I (1993) A human tumor xenograft model of therapy with a bispecific monoclonal antibody targeting c-erbB-2 and CD16. *Cancer Res* 53, 94-100.

22. Galandrini R, Micucci F, Tassi I, Cifone MG, Cinque B, Piccoli M, Frati L & Santoni A (2005) Arf6: a new player in FcgammaRIIIA lymphocyte-mediated cytotoxicity. *Blood* 106, 577-583.

23. Kerr WG & Colucci F (2011) Inositol phospholipid signaling and the biology of natural killer cells. *J Innate Immun* 3, 249-257.

24. Loijens JC & Anderson RA (1996) Type I phosphatidylinositol-4-phosphate 5-kinases are distinct members of this novel lipid kinase family. *J Biol Chem* 271, 32937-32943.

25. Li X, Baskin JG, Mangan EK, Su K, Gibson AW, Ji C, Edberg JC & Kimberly RP (2012) The unique cytoplasmic domain of human FcgammaRIIIA regulates receptor-mediated function. *J Immunol* 189, 4284-4294.

26. Lee SH, Johnson D, Luong R & Sun Z (2015) Crosstalking between androgen and PI3K/AKT signaling pathways in prostate cancer cells. *J Biol Chem* 290, 2759-2768.

27. Manning BD & Toker A (2017) AKT/PKB Signaling: Navigating the Network. *Cell* 169, 381-405.

28. Semenas J, Hedblom A, Miftakhova RR, Sarwar M, Larsson R, Shcherbina L, Johansson ME, Harkonen P, Sterner O & Persson JL (2014) The role of PI3K/AKT-related PIP5K1alpha and the discovery of

its selective inhibitor for treatment of advanced prostate cancer. *Proc Natl Acad Sci U S A* 111, E3689-3698.

29. Choi S, Hedman AC, Sayedyahossein S, Thapa N, Sacks DB & Anderson RA (2016) Agonist-stimulated phosphatidylinositol-3,4,5-trisphosphate generation by scaffolded phosphoinositide kinases. *Nat Cell Biol* 18, 1324-1335.

30. Flemming A (2014) Cancer: Lipid kinase PIP5K1alpha as a new target in prostate cancer. *Nature reviews Drug discovery* 13, 723.

31. Drake JM & Huang J (2014) PIP5K1alpha inhibition as a therapeutic strategy for prostate cancer. *Proc Natl Acad Sci U S A* 111, 12578-12579.

32. Sarwar M, Semenas J, Miftakhova R, Simoulis A, Robinson B, Gjorloff Wingren A, Mongan NP, Heery DM, Johnsson H, Abrahamsson PA, Dizeyi N, Luo J & Persson JL (2016) Targeted suppression of AR-V7 using PIP5K1alpha inhibitor overcomes enzalutamide resistance in prostate cancer cells. *Oncotarget* 7, 63065-63081.

33. Abida W, Cyrta J, Heller G, Prandi D, Armenia J, Coleman I, Cieslik M, Benelli M, Robinson D, Van Allen EM, Sboner A, Fedrizzi T, Mosquera JM, Robinson BD, De Sarkar N, Kunju LP, Tomlins S, Wu YM, Nava Rodrigues D, Loda M, Gopalan A, Reuter VE, Pritchard CC, Mateo J, Bianchini D, Miranda S, Carreira S, Rescigno P, Filipenko J, Vinson J, Montgomery RB, Beltran H, Heath EI, Scher HI, Kantoff PW, Taplin M-E, Schultz N, deBono JS, Demichelis F, Nelson PS, Rubin MA, Chinnaiyan AM & Sawyers CL (2019) Genomic correlates of clinical outcome in advanced prostate cancer. *Proceedings of the National Academy of Sciences* 116, 11428-11436.

34. Abeshouse A, Ahn J, Akbani R, Ally A, Amin S, Andry Christopher D, Annala M, Aprikian A, Armenia J, Arora A, Auman JT, Balasundaram M, Balu S, Barbieri Christopher E, Bauer T, Benz Christopher C, Bergeron A, Beroukhim R, Berrios M, Bivol A, Bodenheimer T, Boice L, Bootwalla Moiz S, Borges dos Reis R, Boutros Paul C, Bowen J, Bowlby R, Boyd J, Bradley Robert K, Breggia A, Brimo F, Bristow Christopher A, Brooks D, Broom Bradley M, Bryce Alan H, Bubley G, Burks E, Butterfield Yaron SN, Button M, Canes D, Carlotti Carlos G, Carlsen R, Carmel M, Carroll Peter R, Carter Scott L, Cartun R, Carver Brett S, Chan June M, Chang Matthew T, Chen Y, Cherniack Andrew D, Chevalier S, Chin L, Cho J, Chu A, Chuah E, Chudamani S, Cibulskis K, Ciriello G, Clarke A, Cooperberg Matthew R, Corcoran Niall M, Costello Anthony J, Cowan J, Crain D, Curley E, David K, Demchok John A, Demichelis F, Dhalla N, Dhir R, Doueik A, Drake B, Dvinge H, Dyakova N, Felau I, Ferguson Martin L, Frazer S, Freedland S, Fu Y, Gabriel Stacey B, Gao J, Gardner J, Gastier-Foster Julie M, Gehlenborg N, Gerken M, Gerstein Mark B, Getz G, Godwin Andrew K, Gopalan A, Graefen M, Graim K, Gribbin T, Guin R, Gupta M, Hadjipanayis A, Haider S, Hamel L, Hayes DN, Heiman David I, Hess J, Hoadley Katherine A, Holbrook Andrea H, Holt Robert A, Holway A,

Hovens Christopher M, Hoyle Alan P, Huang M, Hutter Carolyn M, Ittmann M, Iype L, Jefferys Stuart R, Jones Corbin D, Jones Steven JM, Juhl H, Kahles A, Kane Christopher J, Kasaian K, Kerger M, Khurana E, Kim J, Klein Robert J, Kucherlapati R, Lacombe L, Ladanyi M, Lai Phillip H, Laird Peter W, Lander Eric S, Latour M, Lawrence Michael S, Lau K, LeBien T, Lee D, Lee S, Lehmann K-V, Leraas Kristen M, Leshchiner I, Leung R, Libertino John A, Lichtenberg Tara M, Lin P, Linehan WM, Ling S, Lippman Scott M, Liu J, Liu W, Lochovsky L, Loda M, Logothetis C, Lolla L, Longacre T, Lu Y, Luo J, Ma Y, Mahadeshwar Harshad S, Mallery D, Mariamidze A, Marra Marco A, Mayo M, McCall S, McKercher G, Meng S, Mes-Masson A-M, Merino Maria J, Meyerson M, Mieczkowski Piotr A, Mills Gordon B, Shaw Kenna RM, Minner S, Moinzadeh A, Moore Richard A, Morris S, Morrison C, Mose Lisle E, Mungall Andrew J, Murray Bradley A, Myers Jerome B, Naresh R, Nelson J, Nelson Mark A, Nelson Peter S, Newton Y, Noble Michael S, Noushmehr H, Nykter M, Pantazi A, Parfenov M, Park Peter J, Parker Joel S, Paulauskis J, Penny R, Perou Charles M, Piché A, Pihl T, Pinto Peter A, Prandi D, Protopopov A, Ramirez Nilsa C, Rao A, Rathmell WK, Rätsch G, Ren X, Reuter Victor E, Reynolds Sheila M, Rhie Suhn K, Rieger-Christ K, Roach J, Robertson AG, Robinson B, Rubin Mark A, Saad F, Sadeghi S, Saksena G, Saller C, Salner A, Sanchez-Vega F, Sander C, Sandusky G, Sauter G, Sboner A, Scardino Peter T, Scarlata E, Schein Jacqueline E, Schlomm T, Schmidt Laura S, Schultz N, Schumacher Steven E, Seidman J, Neder L, Seth S, Sharp A, Shelton C, Shelton T, Shen H, Shen R, Sherman M, Sheth M, Shi Y, Shih J, Shmulevich I, Simko J, Simon R, Simons Janae V, Sipahimalani P, Skelly T, Sofia Heidi J, Soloway Matthew G, Song X, Sorcini A, Sougnez C, Stepa S, Stewart C, Stewart J, Stuart Joshua M, Sullivan Travis B, Sun C, Sun H, Tam A, Tan D, Tang J, Tarnuzzer R, Tarvin K, Taylor Barry S, Teebagy P, Tenggara I, Têtu B, Tewari A, Thiessen N, Thompson T, Thorne Leigh B, Tirapelli Daniela P, Tomlins Scott A, Trevisan Felipe A, Troncoso P, True Lawrence D, Tsourlakis Maria C, Tyekucheva S, Van Allen E, Van Den Berg David J, Veluvolu U, Verhaak R, Vocke Cathy D, Voet D, Wan Y, Wang Q, Wang W, Wang Z, Weinhold N, Weinstein John N, Weisenberger Daniel J, Wilkerson Matthew D, Wise L, Witte J, Wu C-C, Wu J, Wu Y, Xu Andrew W, Yadav Shalini S, Yang L, Yang L, Yau C, Ye H, Yena P, Zeng T, Zenklusen Jean C, Zhang H, Zhang J, Zhang J, Zhang W, Zhong Y, Zhu K & Zmuda E (2015) The Molecular Taxonomy of Primary Prostate Cancer. *Cell* 163, 1011-1025.

35. Taylor BS, Schultz N, Hieronymus H, Gopalan A, Xiao Y, Carver BS, Arora VK, Kaushik P, Cerami E, Reva B, Antipin Y, Mitsiades N, Landers T, Dolgalev I, Major JE, Wilson M, Socci ND, Lash AE, Heguy A, Eastham JA, Scher HI, Reuter VE, Scardino PT, Sander C, Sawyers CL & Gerald WL (2010) Integrative genomic profiling of human prostate cancer. *Cancer Cell* 18, 11-22.

36. Beltran H, Prandi D, Mosquera JM, Benelli M, Puca L, Cyrta J, Marotz C, Giannopoulou E, Chakravarthi BV, Varambally S, Tomlins SA, Nanus DM, Tagawa ST, Van Allen EM, Elemento O, Sboner A,

Garraway LA, Rubin MA & Demichelis F (2016) Divergent clonal evolution of castration-resistant neuroendocrine prostate cancer. *Nat Med* 22, 298-305.

37. Gao J, Aksoy BA, Dogrusoz U, Dresdner G, Gross B, Sumer SO, Sun Y, Jacobsen A, Sinha R, Larsson E, Cerami E, Sander C & Schultz N (2013) Integrative analysis of complex cancer genomics and clinical profiles using the cBioPortal. *Sci Signal* 6, pl1.

38. Cerami E, Gao J, Dogrusoz U, Gross BE, Sumer SO, Aksoy BA, Jacobsen A, Byrne CJ, Heuer ML, Larsson E, Antipin Y, Reva B, Goldberg AP, Sander C & Schultz N (2012) The cBio cancer genomics portal: an open platform for exploring multidimensional cancer genomics data. *Cancer Discov* 2, 401-404.

39. Wegiel B, Bjartell A, Tuomela J, Dizeyi N, Tinzl M, Helczynski L, Nilsson E, Otterbein LE, Harkonen P & Persson JL (2008) Multiple cellular mechanisms related to cyclin A1 in prostate cancer invasion and metastasis. *J Natl Cancer Inst* 100, 1022-1036.

40. Miftakhova R, Hedblom A, Semenas J, Robinson B, Simoulis A, Malm J, Rizvanov A, Heery DM, Mongan NP, Maitland NJ, Allegrucci C & Persson JL (2016) Cyclin A1 and P450 Aromatase Promote Metastatic Homing and Growth of Stem-like Prostate Cancer Cells in the Bone Marrow. *Cancer research* 76, 2453-2464.

41. Larsson P, Syed Khaja AS, Semenas J, Wang T, Sarwar M, Dizeyi N, Simoulis A, Hedblom A, Wai SN, Ødum N & Persson JL (2020) The functional interlink between AR and MMP9/VEGF signaling axis is mediated through PIP5K1α/pAKT in prostate cancer. *International Journal of Cancer* 146, 1686-1699.

42. Armenia J, Wankowicz SAM, Liu D, Gao J, Kundra R, Reznik E, Chatila WK, Chakravarty D, Han GC, Coleman I, Montgomery B, Pritchard C, Morrissey C, Barbieri CE, Beltran H, Sboner A, Zafeiriou Z, Miranda S, Bielski CM, Penson AV, Tolonen C, Huang FW, Robinson D, Wu YM, Lonigro R, Garraway LA, Demichelis F, Kantoff PW, Taplin M-E, Abida W, Taylor BS, Scher HI, Nelson PS, de Bono JS, Rubin MA, Sawyers CL, Chinnaiyan AM, Schultz N, Van Allen EM & Team PSCIPCD (2018) The long tail of oncogenic drivers in prostate cancer. *Nature Genetics* 50, 645-651.

43. Larsson P, Syed Khaja AS, Semenas J, Wang T, Sarwar M, Dizeyi N, Simoulis A, Hedblom A, Wai SN, Odum N & Persson JL (2019) The functional interlink between AR and MMP9/VEGF signaling axis is mediated through PIP5K1alpha/pAKT in prostate cancer. *Int J Cancer*.

44. Galandrini R, Tassi I, Mattia G, Lenti L, Piccoli M, Frati L & Santoni A (2002) SH2-containing inositol phosphatase (SHIP-1) transiently translocates to raft domains and modulates CD16-mediated cytotoxicity in human NK cells. *Blood* 100, 4581-4589.

Supplemental Information

Table 1.

Correlations for protein expression in patient samples

Supplemental Figure 1. In the MSKCC/DFCI patient cohort consisting primary PCa (n=1013 PCa cases) from the Prostate Oncogenenome Project dataset in cBioPortal databases, *FCGR3A* gene alterations were found in 3% of PCa cases, which was similar to *PIP5K1A* gene alterations accounted for 5% in this PCa cohort.

Supplemental Figure 2. Dot plots graph shows the correlations between AR and FcγRIIIa mRNA expression in log 2 by using the SU2C/PCF metastatic PCa cohort (n=429). The R2 vaule and p value are indicated.

Supplemental Figure 3. Dot plots graph shows the correlations between AR and FcγRIIIa mRNA expression in log 2 by using the TCGA PCa cohort (n=333). The R2 vaule and p value are indicated.

Supplemental Figure 4: Expression of FcγRIIIa in PC-3 cells and U-937 cells. (a). Semi-quantitative RT-PCR using the primers specific for *FCGR3A* was performed. The PCR-product of *FCGR3A* in mono-cultured PC-3 cells, U-937 cells and PC-3 after co-culturing with U-937 cells, the cells from each condition were collected after 48 hours in the culture. (b). The sequence alignment of the PCR-product of *FCGR3A* from PC-3 cells with the consensus sequence from NCBI is shown.

Supplemental Figure 5. FcγRIIIa protein expression in PC-3 cells along with various types of PCa cell lines by using immunoblot analysis. U-937 monocytes and PCa cell lines including C4-2, VCaP, PC-3 and PC-3M cells were subjected to the immunoblotting analysis. Antibodies against FcγRIIIa and GAPDH were used.

Supplemental Figure 6. The effect of AR overexpression on FCGR3A mRNA expression. AR overexpression was induced in LNCaP cells by transfecting the cells with a vector carrying full-length AR or a control vector. The semi-quantitative RT-PCR analysis using the primers specific for FCGR3A was performed.

Supplemental Figure 7. The effect of AR inhibition on FCGR3A mRNA expression. LNCaP cells were treated with enzalutamide for 6 hours, 12 hours and 24 hours respectively. The effect of AR inhibition by enzalutamide on the expression of AR was measured by quantitative RT-PCR.

Figures and legends

Figure 1. Evaluation of FcγRIIIa expression in primary tumors and metastatic lesions from PCa patients and the association between FcγRIIIa expression and patient outcome.

(a). Representative microphotographs of benign prostate hyperplasia (BPH) (n=48), PCa specimens (PCa) (n=52) and metastatic lesions in bone marrow (BM mets), lymph node (LN mets), and lung (Lung mets) from PCa patients (n=19), as assessed by immunohistochemical analysis of TMAs using antibody against FcγRIIIa.The scale bars: 300 μm and 50 μm are indicated and apply to all images in the panel. (b) Box-plot quantitative comparison of FcγRIIIa protein expression between primary PCa, n=52 and metastatic PCa, n=19 (mean scores in primary and metastatic lesions were 1.73 and 2.17, difference=0.74; 95%CI=1.81-2.27, p=0.006). **p <0.01 is indicated. The error bars indicate SD. The student t test was used to determine the significance. (c) Box-plot quantitative comparison of FCGR3A mRNA expression between primary (n=131) and metastatic lesions (n=19) (p<0.01), **p <0.01 is indicated. The error bars indicate SD. The student t test was used to determine the significance. (d). Kaplan-Meier survival analysis based on Biochemical Recurrence-free (BCR-free) survival shows the difference between patients with low and high expression of FCGR3A. Differences in BCR-free survival between two groups and p values were calculated using the log-rank test. P= 0.026 is indicated. (e). Alterations in genes and mRNA expression of FCGR3A, AR and PIP5K1A and PTEN in metastatic PCa cohort SU2C/PCF (n=429) are shown in onco-prints. Different types of alterations in genes and their respective mRNA expression are indicated. (f). Dot plots graph shows the FCGR3A mRNA

expression in four subgroups of PCa that were categorized using Gleason scores (TCGA PCa cohort, n=333). Subgroups with Gleason score 3+3 (n=65), Gleason score 3+4 (n=102), Gleason score 4+3 (n=78) and Gleason score >=8 (n=88). The expression of FCGR3A mRNA in comparison between group of Gleason score >=8 and Gleason score 3+4, p=0.003; the expression of FCGR3A in comparison between group of Gleason score 4+3 and Gleason score 3+3, p<0.001. The ANOVA test was used to determine the significance. (g). Alterations in genes and mRNA expression of FCGR3A and AR in the PCa cohort mentioned in (f) are shown in onco-prints.

Figure 2. The role of FcγRIIIa in promoting tumorigenesis and its association with AR and PIP5K1α in C4-2 cells.

(a). Immunoblot analysis was performed to confirm the induced overexpression of FcγRIIIa in C4-2 cells that were transfected with pLX304-FCGR3A vector (FcγRIIIa) as compared with C4-2 cells that were transfected with pLX304 control vector (Ctrl). The quantifications of the immunoblots are shown in the right panels. Data is presented as average of three independent experiments (n=3), p<0.05, as indicated by "*". The error bars indicate SEM. The student t test was used to determine the significance. (b). The effect of FcγRIIIa overexpression on the tumorigenic ability of C4-2 cells was assessed using tumor-spheroid formation assays. Data is presented as average of three independent experiments (n=3), p<0.05, as indicated by "*". The error bars indicate SEM. The student t test was used to determine the significance. (c). The effect of DHT treatment on FcγRIIIa and AR expression in C4-2 cells was examined by using immunoblot analysis. C4-2 cells treated with 0.1% DMSO as vehicle control (Ctrl) and C4-2 cells treated with DHT at 5 nM (DHT) for 12 hours are indicated. Data is representative of two independent experiments (n=2) with each experiment performed in triplicates (n=3). (d and e). The effect of FcγRIIIa overexpression on AR and PIP5K1α expression in C4-2 cells was assessed using immunoblot analysis. The data are representative of three independent experiments (n=3). (f). The effect of siRNA-mediated knockdown of FcγRIIIa on AR and PIP5K1α expression in C4-2 cells was assessed using immunoblot analysis. C4-2 cells transfected with siRNA scramble control (ctrl) or siRNA to FcγRIIIa (FcγRIIIa) are indicated. Three independent experiments (n=3) were performed. (g). The quantifications of the immunoblots of FcγRIIIa and AR are shown. Data is presented as average of three independent experiments (n=3), p<0.05, as indicated by "*". The error bars indicate SEM. The student t test was used to determine the significance. (h). The formation of protein complexes among FcγRIIIa, PIP5K1α and AR was assessed by using

immunoprecipitation (IP) assay. C4-2 cells were subjected to immunoprecipitation (IP) assay in which antibody against PIP5K1α was used to pull down the immuno-complexes, and antibody to IgG was used as a negative control. Antibodies against FcγRIIIa and AR were used for immunoblot analysis (IB). The equal amount of total lysates was used as input control for immunoblot analysis of the immuno-precipitated protein lysates. Data is representative of at least two independent experiments (n=2). (i). Immunofluorescence analysis was performed to assess the subcellular localization and its co-localization with PIP5K1α. Representative images of the subcellular localizations of FcγRIIIa expression (red), PIP5K1α (green) and overlapped image (Merged) are shown. The scale bar: 20 μm is indicated. Data is representative of four independent experiments (n=4).

Figure 3. The association between AR and FcγRIIIa in LNCaP cells.

(a). The effect of elevated level of AR expression on FcγRIIIa and PSA protein expression in LNaCp cells was assessed using immunoblot analysis. The quantifications of the immunoblots for AR and FcγRIIIa are shown in the right panels. Expression of AR and FcγRIIIa was significantly higher in LNCaP cells transfected with PCMV-AR vector than that of control pCMV vector, for AR, p=0.003, for FcγRIIIa, p=0.03. Data is presented as average of three independent experiments (n=3), $^{**}P<0.01$ and $^{*}p<0.05$ are indicated. The error bars indicate SEM. The student t test was used to determine the significance. (b). The effect of inhibition of AR using enzalutamide on FcγRIIIa expression in LNCaP cells was assessed using immunoblot analysis. Data is representative of two independent experiments (n=2) with each experiment performed in duplicates (n=2). (c and d). The quantifications of the immunoblots for AR and FcγRIIIa are shown. Data is presented as average of two independent experiments (n=2) with each experiment performed in duplicates (n=2), $p<0.05$, as indicated by "*". $p<0.01$ is indicated by "**". Expression of AR and FcγRIIIa was significantly decreased in LNCaP cells treated with enzalutamide for 12 hours and 24 hours respectively as compared with that of vehicle control treated cells (for AR, enzalutamide treatment vs. control treatment for 6 hours, p=0.026; 12 hours, p=0.003 and 24 hours, p=0.021; for FcγRIIIa, enzalutamide treatment vs. control treatment for 6 hours, p=0.325, 12 hours, p=0.03 and 24 hours, p=0.034.), The error bars indicate SEM. The student t test was used to determine the significance.

Figure 4. The role of FcγRIIIa in promoting tumorigenesis and its association with AR and PIP5K1α in PC-3 cells.

(a). The effect of induced overexpression of FcγRIIIa on expression of PIP5K1α in PC-3 was assessed by immunoblot analysis. The quantifications of the immunoblots are shown in the right panels. Expression of FcγRIIIa and PIP5K1α was significantly higher in PC-3 cells transfected with FcγRIIIa than that of control vector, for PIP5K1α, p=0.011. Data is representative of three independent experiments (n=3), p<0.05, as indicated by "*". The error bars indicate SEM. The student t test was used to determine the significance. (b). The effect of FcγRIIIa overexpression on the tumorigenic ability of PC-3 cells was assessed using tumor-spheroid formation assays. Data shown is representative of two independent experiments (n=2) with each experiment performed in triplicates (n=3), p<0.05, as indicated by "*". The error bars indicate SEM. The student t test was used to determine the significance. (c). The effect of induced overexpression of FcγRIIIa on migratory ability of PC-3 cells was assessed by using migration assay. Data shown is presented as average of three independent experiments (n=3), p<0.01, as indicated by "**". The error bars indicate SEM. The student t test was used to determine the significance. (d). The depletion of FcγRIIIα in PC-3 cells transfected with siFcγRIIIa RNA (FcγRIIIa) compared with PC-3 cells transfected with si-RNA scramble control (Ctrl) was assessed by using immunoblot analysis. Data is representative of two independent experiments (n=2) with each experiment performed in duplicates (n=2). (e). The effect of FcγRIIIa knockdown on tumorigenic ability of PC-3 cells was determined using tumor-spheroid formation assays. Representative images of tumor spheroids are shown. The spheroid counts are shown in the right panel. Mean tumor-spheroid counts in si-control and si-FcγRIIIa PC-3 cells were 56 and 14, difference=42, 95% CI in si-control=43-68 and si- FcγRIIIa=6-21, p=0.012. Data is representative of two independent experiments (n=2), each experiment was performed in triplicates (n=3), p<0.05, as indicated by "*". The error bars indicate SEM. The student t test was used to determine the significance. (f). The effect of FcγRIIIa knockdown on PIP5K1α in PC-3 cells was determined using immunoblot analysis. Data shown in the right panel is representative of three independent experiments (n=3), p<0.05, as indicated by "*". The error bars indicate SEM. The student t test was used to determine the significance. (g). The effect of inhibition of PIP5K1α by its inhibitor ISA-2011B on IP5K1α, FcγRIIIa and pAKT in PC-3 cells was determined using immunoblot analysis. Data is representative of at least three independent experiments (n=3). (h). Effect of induced AR alone or together with induced FcγRIIIa or PIP5K1α expression on the activity of full-length cyclin A1 promoter was assessed using

luciferase assay. The vectors were induced together with luc-reporter vector "Luc" or cyclin A1 promoter-luc reporter vector "A1 Luc" into PC-3 cells (For AR alone, p=0.003, for AR+PIP5K1α, p=0.008*)*. Data is representative of at least two independent experiments (n=2), and each experiment was performed in triplicates (n=3). The error bars indicate SEM. The student t test was used to determine the significance. (i). Effect of FcγRIIIa overexpression on androgen responsive (ARE) promoter activity in LNCaP cells was carried out using the dual-luciferase assays. FcγRIIIa overexpression induced ARE reporter luciferase activity led to an increase by 100% relative to controls in LNCaP cells, p=0.013. Data shown is presented as average of two independent experiments (n=2), and each experiment was performed in triplicates, $p<0.05$, as indicated by "*". The error bars indicate SEM. The student t test was used to determine the significance.

Figure 5. The inhibitory effect of FcγRIIIa knockdown on growth of tumors in xenograft mouse model. (a). Growth curves of PC-3M tumors expressing si-control RNA (siCtrl) or si-FcγRIIIa (FcγRIIIa) in xenograft mice are shown (n=4 per group). Tumor volumes are indicated in Y-axis and the measurement days are indicated in x-axis. Tumors from each group were collected at the end of the experiment. (b, c, d, e, f). Expression of the key proteins for proliferation and invasion in the xenograft tumors collected from the mice was assessed by using immunohistochemical analysis. Representative images of the siCtrl tumors and si-FcγRIIIa tumors that were stained with antibodies against Ki-67, PIP5K1α, pAKT, MMP9 and VEGFR2 are shown. Quantification of the staining intensity of the proteins are shown in the right panels. Mean Ki-67 positive cells in siCtrl and siFCGR3A tumors were 71.82% and 46.67%, difference=25.15%; 95% CI=38.40 to 54.93%, $p<0.001$. Mean PIP5K1α expression in si-control and si-FcγRIIIa tumors were 2.82 and 2.20, difference=0.54, 95% CI for si-control=2,78-2,85, si-FcγRIIIa =2.13-2.43. p=0.048; mean pAKT expression for si-control and si-FcγRIIIa were 2.34 and 1.96, difference=0.39, 95% CI for si-control=2.3-2.38, and for si-FcγRIIIa =1.94-1.98, p=0.0045. Mean MMP9 expression in si-control and si-FcγRIIIa were 1.82 and 1.44, difference=0.37, 95% CI in si-control=1.8-1.84, and in si-FcγRIIIa=1.39-1.5, p=0.028. $^{**}P<0.01$ and $^{*}p<0.05$ are indicated. Tumors from the two groups (for si-control group, n=3; for si-FcγRIIIa group, n=2) were stained with the indicated antibodies and were evaluated. The error bars indicate SEM. The student t test was used to determine the significance. The scale bars: 2 mm and 100 μm in the imges in b, c, d, e and f are indicated. (g) Representative images of the lymph nodes containing metastatic lesions from the xenograft mice bearing si-FcγRIIIa tumors as compared

with that of si-control RNA (siCtrl) are shown. Tumors were immune-stained with the antibodies against CD19 and Vimentin that are markers for cancer cells. Tumor cells positive to the markers were indicated by the arrows. Tumors from the two groups (for si-control group, n=3; for si-FcγRIIIa group, n=2) were stained with the indicated antibodies and were evaluated. The scale bars: 1 mm and 100 μm are indicated.

Figure 6. The inter-link between PIP5K1α and FcγRIIIa and inhibition of via monocloncal antibody M3G8 in PCa cells.

(a). The effect of M3G8 on growth of tumor-spheroids derived from PC-3 cells co-cultured with U-937 cells. Tumor-spheroids were treated with control or M3G8 antibodies. Mean tumor-spheroids counts in control antibody-treated and in M3G8-treated groups= 38-26, difference=12, 95%CI=22-31, p=0.028. Data is representative of two independent experiments (n=2), and each experiment was performed in triplicates, $p<0.05$, as indicated by "*". The error bars indicate SEM. The student t test was used to determine the significance. (b). Representative immunofluorescent images from (a) showing the tumor-spheroids treated with M3G8 or control antibodies that are highlighted with phalloidin-staining (red). The experiments were replicated (n=2). The scale bar: 20 μm is indicated. (c) Growth of PC-3 subcutaneous xenograft tumors that were treated with control IgG antibody (Ctrl) or M3G8 antibody. Treatment started on day 0 when the mean tumor volume reached to over 300 mm^3 and ended on day 21 (n =3-4 mice per group). Y-axis indicates tumor volumes and x-axis indicates days of treatment. P=0.012. *$p<0.05$ is indicated. (d and e) Immunohistochemical analysis of the xenograft tumors from mice treated with control antibody or M3G8 antibody. Representative microphotographs of images showing expression of PIP5K1α and VEGFR2 are shown in left panels and quantification of the staining intensity of the antibodies against these proteins in tumor cells are in shown in the right panels. Mean PIP5K1α expression in control-treated and M3G8-treated were 2.63 and 1.0, difference = 1.63, 95%Cl for control-treated= 2.49-2.76 and for M3G8-treated= 0.72-1.28, p= 0.01. Mean VEGFR2 expression in control-treated and M3G8-treated= 3.0 and 1.08, difference = 1.92, 95% Cl for M3G8-treated= 0.77-1.4, p = 0.01). Tumors from the two groups (n=3) were stained with the indicated antibodies and were evaluated. *$p<0.05$ is indicated. The error bars indicate SEM. The student t test was used to determine the significance. The scale bars: 50 μm is indicated.

Figure 7. The effect of M3G8 on tumor growth and metastasis in xenograft mouse models.

(a). Schematic illustration depicts the experimental procedures of establishment of distant metastasis including bone metastasis by using tumor-spheroids derived from $ALDH^{high}$ PC-3M cells, and *in vivo* treatment regimens using M3G8 antibody. (b). Representative images to show the bioluminescent *in vivo* imaging on visualization of tumor metastasis in mice bearing metastasis and were treated with M3G8 or control antibodies. The signals were obtained by using flourochrome-conjugated HLA-ABC antibody which was injected into the mice 6 hours before applying mice on the IVIS imaging device. (c). Mean metastatic areas and intensity in pixels for Ctrl group (n=4) and M3G8 group (n=3) are shown. On day 0, p=0.8257. On day 15 post-treatment, mean value of metastatic areas plus signal intensity for control-treated and M3G8-treated groups were 250 and 76, difference= 174, 95% CI for control group= 185-310, and for M3G8 group= 0-157, p=0.039. The error bars indicate SEM. The student t test was used to determine the significance. (d). Representative microphotographs showing CK19-positive cells in the bone marrow, indicating bone metastasis. Quantification of the staining intensity of CK19 in the bone marrow of the mice (n=2-3) that were treated with Ctrl or M3G8 is shown in the right panel. The arrow heads point to the CK19-positive tumor cells or tumor cell clusters. *p<0.05 is indicated. The student t test was used to determine the significance. The scale bar: 50 μm is indicated. (e). The effect of M3G8 and ISA-2011B alone or in combination on the migratory ability of C4-2 cells was assessed by using the migration assays. After treatment with the agents, the equal amount of the cells from different groups were subjected to the boyden chamber migration assay for 18 hours. M3G8 treatment or ISA-2011B treatment alone reduced migratory ability of C4-2 cells as compared with that of controls (for M3G8, *p=0.016*; for ISA-2011B, *p=0.006*). Combination of M3G8 and ISA-2011B reduced the migratory ability of the cells as compared with that of controls (p=0.003). Data is presented as average of two independent experiments (n=2). **P<0.01 and *p<0.05 are indicated. The error bars indicate SEM. The student t test was used to determine the significance.

Table 1.

Correlations for protein expression in patient samples

FcγRIIIa and PIP5K1α		FcγRIIIa and Cyclin A1	
r^2	*p*-value	r^2	*p*-value
0.480	<0.000	0.334	0.001

Figure 1

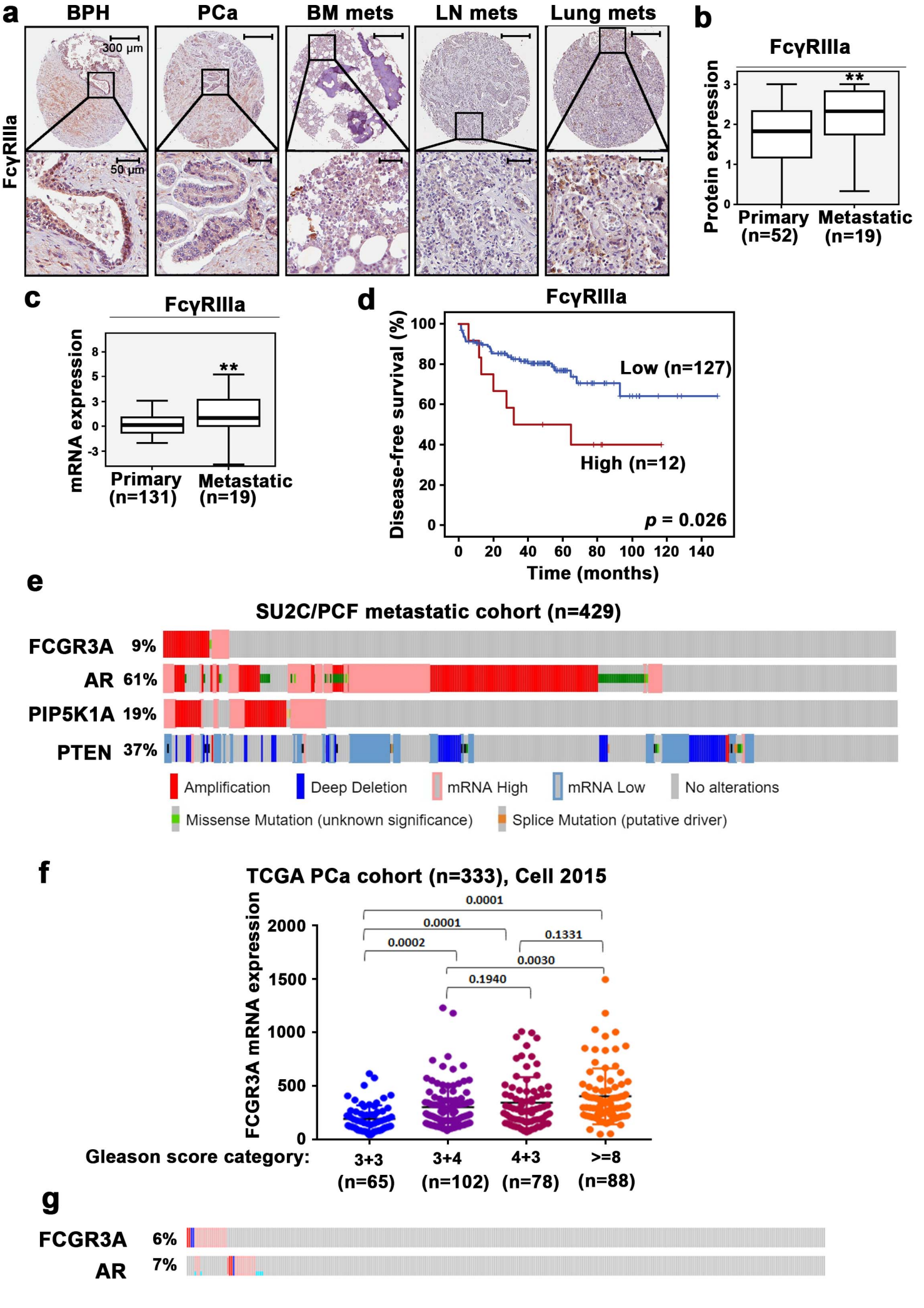
a
BPH
PCa
BM mets
LN mets
Lung mets
FcγRIIIa
300 μm
50 μm
b
FcγRIIIa
Protein expression
**
Primary (n=52)
Metastatic (n=19)
c
FcγRIIIa
mRNA expression
**
Primary (n=131)
Metastatic (n=19)
d
FcγRIIIa
Disease-free survival (%)
Low (n=127)
High (n=12)
p = 0.026
Time (months)
e
SU2C/PCF metastatic cohort (n=429)
FCGR3A 9%
AR 61%
PIP5K1A 19%
PTEN 37%
Amplification
Deep Deletion
mRNA High
mRNA Low
No alterations
Missense Mutation (unknown significance)
Splice Mutation (putative driver)
f
TCGA PCa cohort (n=333), Cell 2015
FCGR3A mRNA expression
0.0001
0.0001
0.0002
0.1331
0.0030
0.1940
Gleason score category:
3+3 (n=65)
3+4 (n=102)
4+3 (n=78)
>=8 (n=88)
g
FCGR3A 6%
AR 7%

Figure 2

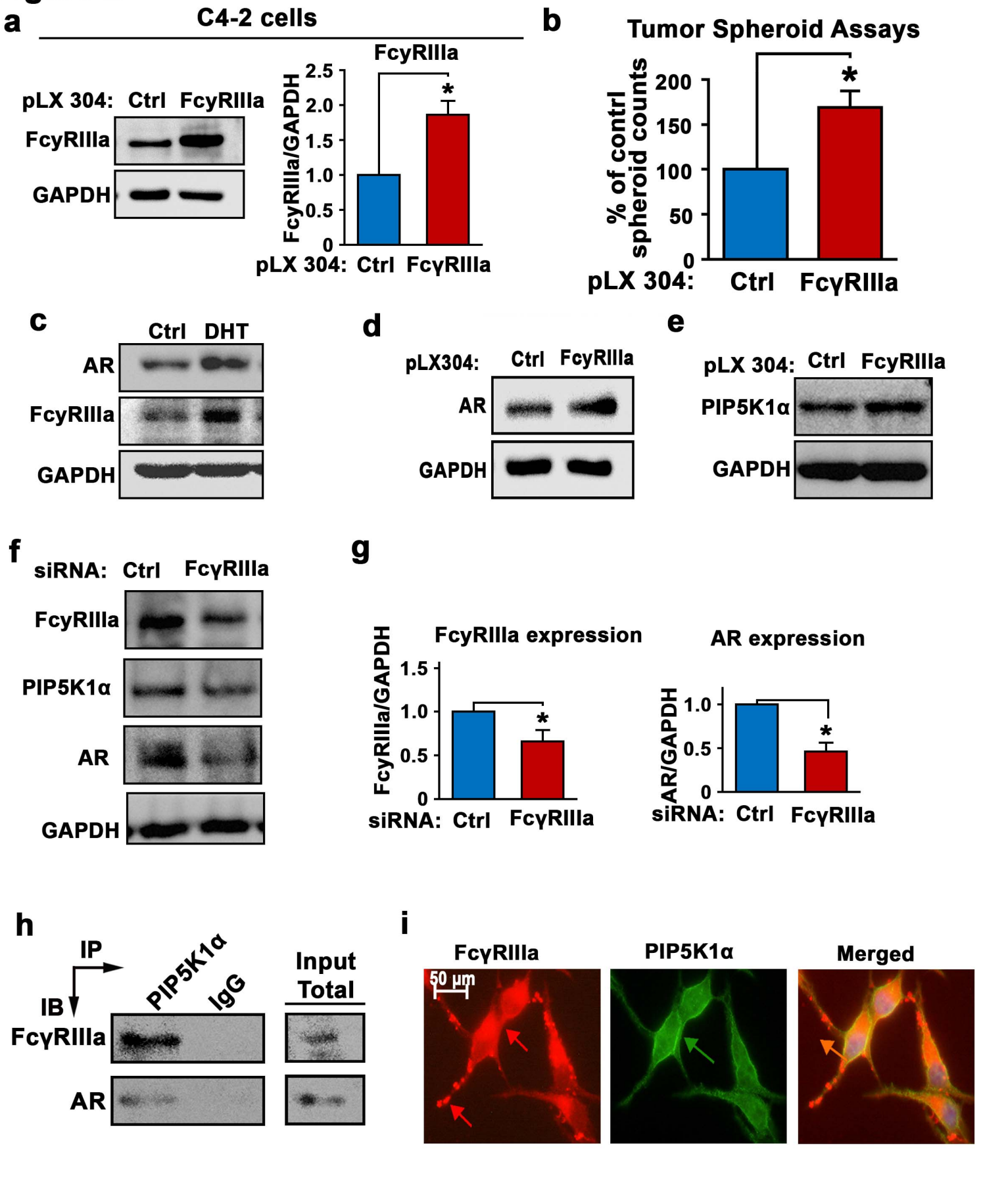
a
C4-2 cells
pLX 304: Ctrl FcγRIIIa
FcγRIIIa
GAPDH
FcγRIIIa/GAPDH
2.5
2.0
1.5
1.0
0.5
0
*
pLX 304: Ctrl FcγRIIIa
b
Tumor Spheroid Assays
% of contrl spheroid counts
200
150
100
50
0
*
pLX 304: Ctrl FcγRIIIa
c
Ctrl DHT
AR
FcγRIIIa
GAPDH
d
pLX304: Ctrl FcγRIIIa
AR
GAPDH
e
pLX 304: Ctrl FcγRIIIa
PIP5K1α
GAPDH
f
siRNA: Ctrl FcγRIIIa
FcγRIIIa
PIP5K1α
AR
GAPDH
g
FcγRIIIa expression
FcγRIIIa/GAPDH
1.5
1.0
0.5
0
*
siRNA: Ctrl FcγRIIIa
AR expression
AR/GAPDH
1.0
0.5
0
*
siRNA: Ctrl FcγRIIIa
h
IP
IB
PIP5K1α
IgG
Input Total
FcγRIIIa
AR
i
FcγRIIIa
PIP5K1α
Merged
50 μm

Figure 3

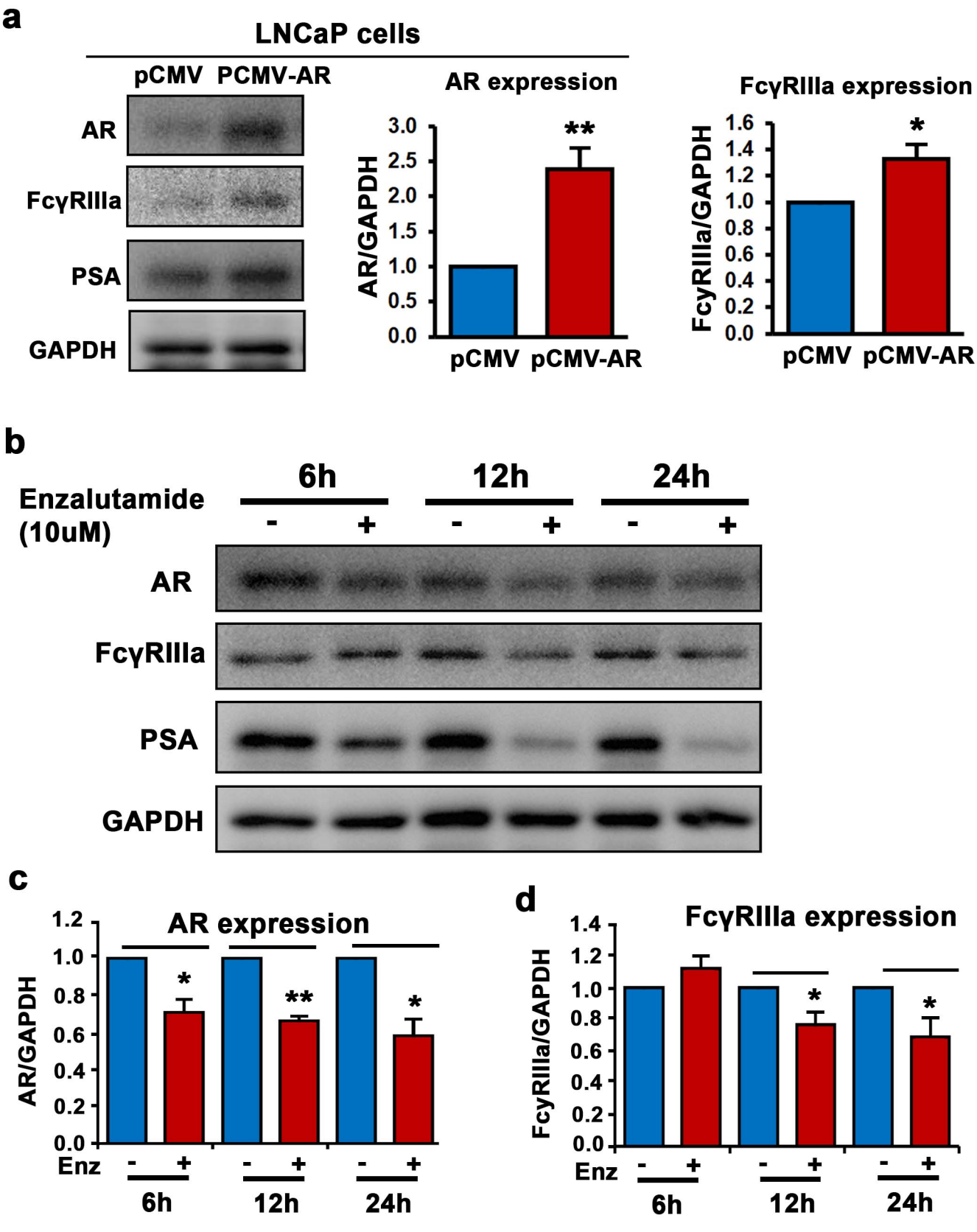
a
LNCaP cells
pCMV PCMV-AR
AR
FcγRIIIa
PSA
GAPDH
AR expression
AR/GAPDH
3.0
2.5
2.0
1.5
1.0
0.5
0.0
**
pCMV pCMV-AR
FcγRIIIa expression
FcγRIIIa/GAPDH
1.6
1.4
1.2
1.0
0.8
0.6
0.4
0.2
0.0
*
pCMV pCMV-AR
b
Enzalutamide (10uM)
6h
12h
24h
- + - + - +
AR
FcγRIIIa
PSA
GAPDH
c
AR expression
AR/GAPDH
1.2
1.0
0.8
0.6
0.4
0.2
0.0
* ** *
Enz - + - + - +
6h 12h 24h
d
FcγRIIIa expression
FcγRIIIa/GAPDH
1.4
1.2
1.0
0.8
0.6
0.4
0.2
0.0
* *
Enz - + - + - +
6h 12h 24h

a
PC-3 cells
pLX 304: Ctrl FcγRIIIa
FcγRIIIa
PIP5K1α
GAPDH
FcγRIIIa/GAPDH
PIP5K1α/GAPDH
2.0
1.5
1.0
0.5
0
*
pLX 304: Ctrl FcγRIIIa
Ctrl FcγRIIIa
b
Tumor Spheroid Assays
% of spheroids relative of control
250
200
150
100
50
0
*
pLX 304: Ctrl FcγRIIIa
c
Migration assay
Migrated cells (% of Control)
250
200
150
100
50
0
**
pLX 304: Ctrl FcγRIIIa
d
siRNA: Ctrl FcγRIIIa
FcγRIIIa
GAPDH
e
Tumor Spheroid Assays
siRNA: Ctrl FcγRIIIa
% of spheroids relative of control
100
75
50
25
0
*
siRNA: Ctrl FcγRIIIa
f
siRNA: Ctrl FcγRIIIa
PIP5K1α
GAPDH
PIP5K1α/GAPDH
1.0
0.5
0
PIP5K1α
*
siRNA: Ctrl FcγRIIIa
g
PC-3 cells
ISA-2011B: - +
PIP5K1α
FcγRIIIa
pAKT
β-Actin
h
PC-3 cells
Promoter Activation Assay
Relative to Luc control (%)
900
800
700
600
500
400
300
200
100
0
Luc
Ctrl Luc
Luc
Cyclin A1promoter
*
*
Contrl
AR
Contrl
AR
AR+ FcγRIIIa
AR+ PIP5K1α
Luc
A1 Luc
i
LNCaP cells
ARE Activation Assay
LUC
promoter-ARE reporter
Relative Luc activity to control(%)
1200
1000
800
600
400
200
0
*
Ctrl FcγRIIIa

Figure 5

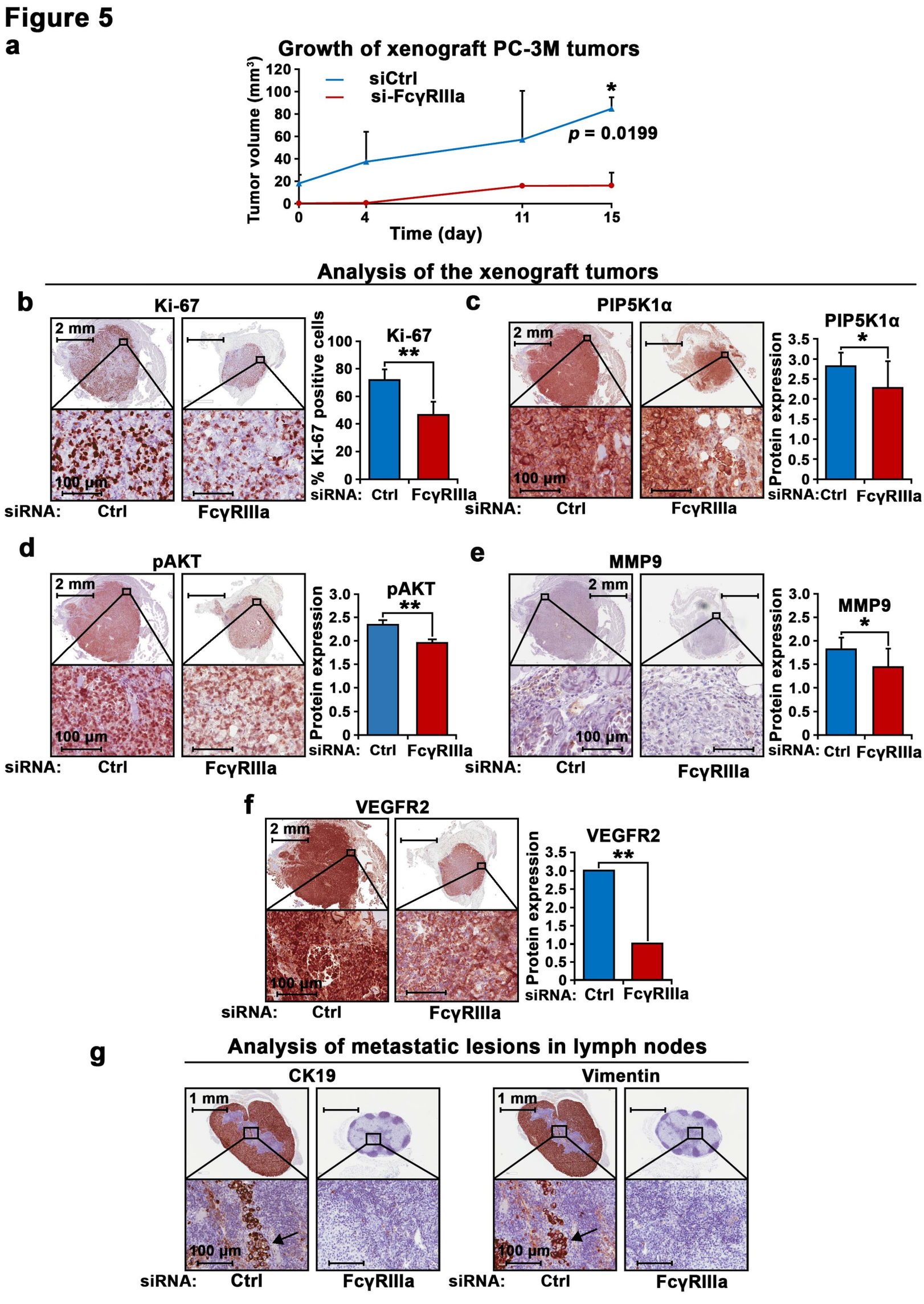
a
Growth of xenograft PC-3M tumors
siCtrl
si-FcγRIIIa
Tumor volume (mm3)
Time (day)
p = 0.0199
Analysis of the xenograft tumors
b
Ki-67
2 mm
100 μm
siRNA: Ctrl FcγRIIIa
% Ki-67 positive cells
c
PIP5K1α
Protein expression
d
pAKT
e
MMP9
f
VEGFR2
g
Analysis of metastatic lesions in lymph nodes
CK19
Vimentin
1 mm

Figure 6

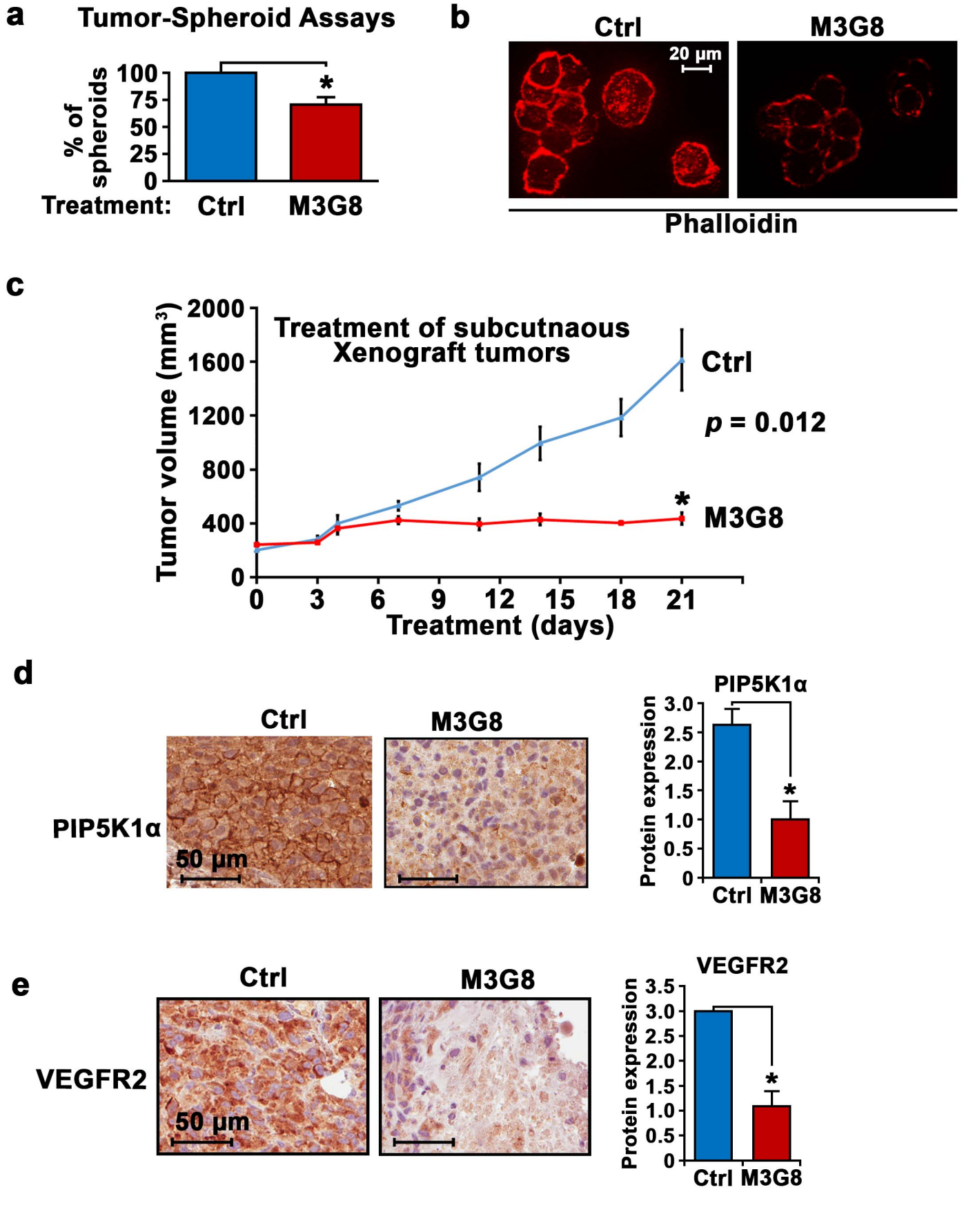
a
Tumor-Spheroid Assays
% of spheroids
100
75
50
25
0
*
Treatment:
Ctrl
M3G8
b
Ctrl
M3G8
20 μm
Phalloidin
c
Treatment of subcutnaous Xenograft tumors
Tumor volume (mm³)
2000
1600
1200
800
400
0
0
3
6
9
12
15
18
21
Treatment (days)
Ctrl
p = 0.012
*
M3G8
d
PIP5K1α
Ctrl
M3G8
50 μm
PIP5K1α
Protein expression
3.0
2.5
2.0
1.5
1.0
0.5
0
*
Ctrl
M3G8
e
VEGFR2
Ctrl
M3G8
50 μm
VEGFR2
Protein expression
3.5
3.0
2.5
2.0
1.5
1.0
0.5
0
*
Ctrl
M3G8

Figure 7

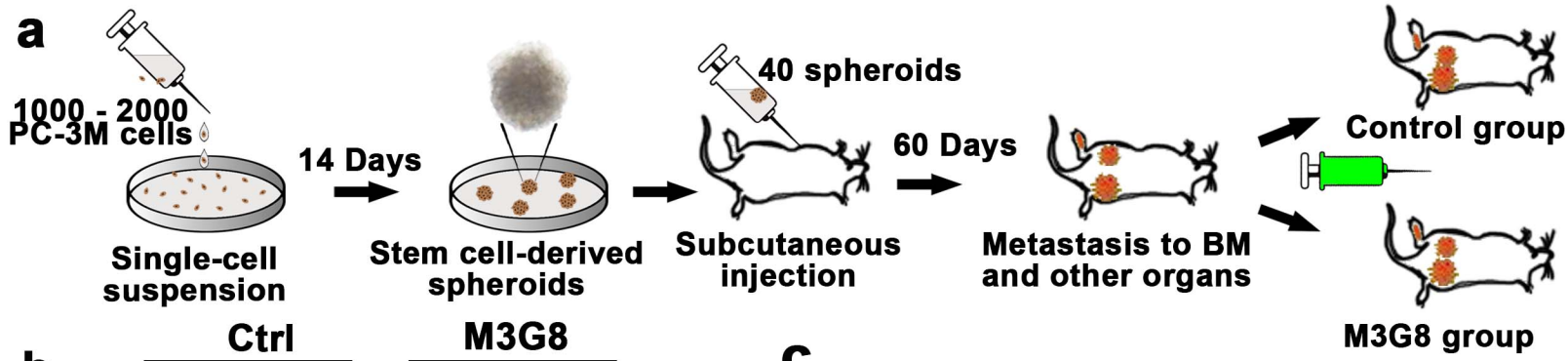
a
1000 - 2000
PC-3M cells
Single-cell
suspension
14 Days
Stem cell-derived
spheroids
40 spheroids
Subcutaneous
injection
60 Days
Metastasis to BM
and other organs
Control group
M3G8 group

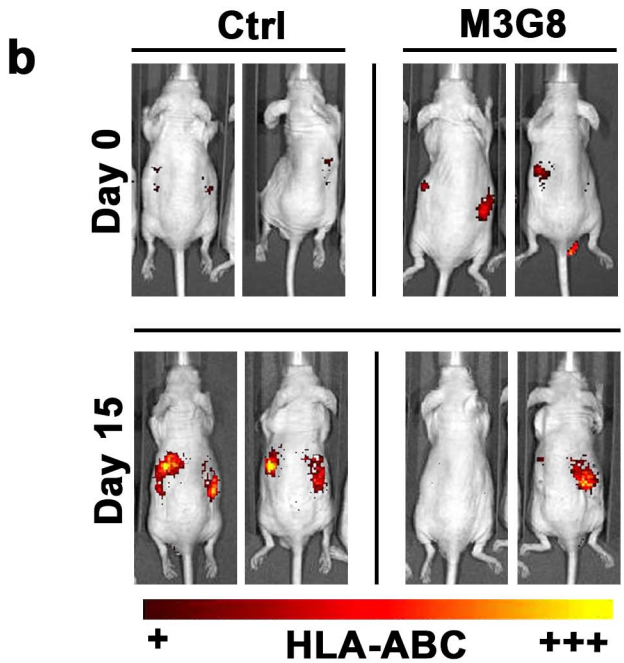
b
Ctrl
M3G8
Day 0
Day 15
+
HLA-ABC
+++

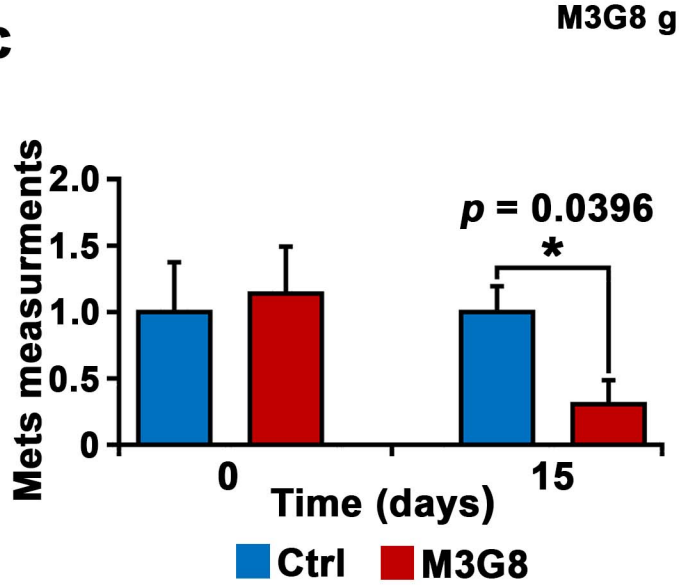
c
Mets measurments
2.0
1.5
1.0
0.5
0
p = 0.0396
*
0
15
Time (days)
Ctrl
M3G8

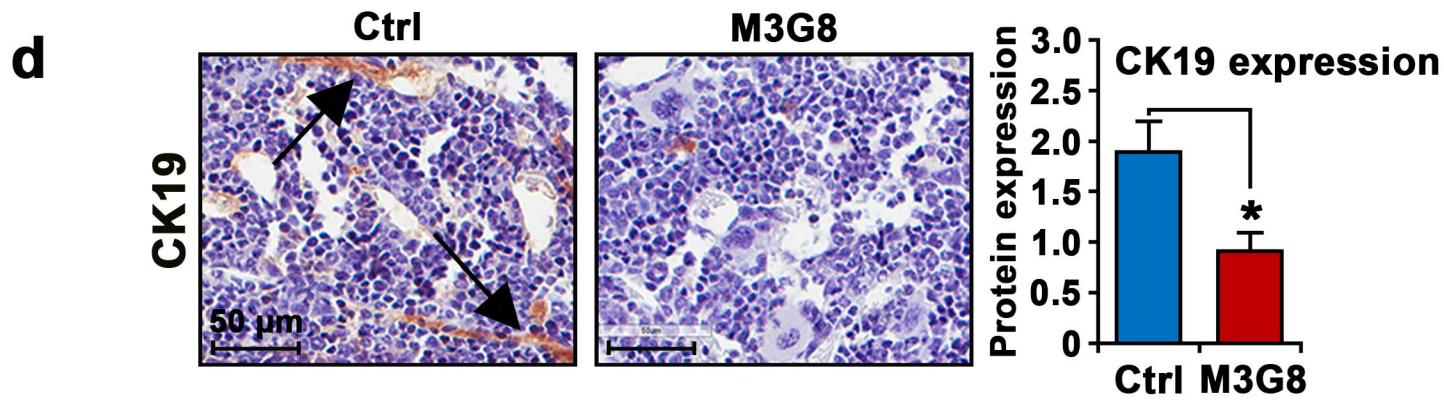
d
Ctrl
M3G8
CK19
50 µm
CK19 expression
Protein expression
3.0
2.5
2.0
1.5
1.0
0.5
0
*
Ctrl
M3G8

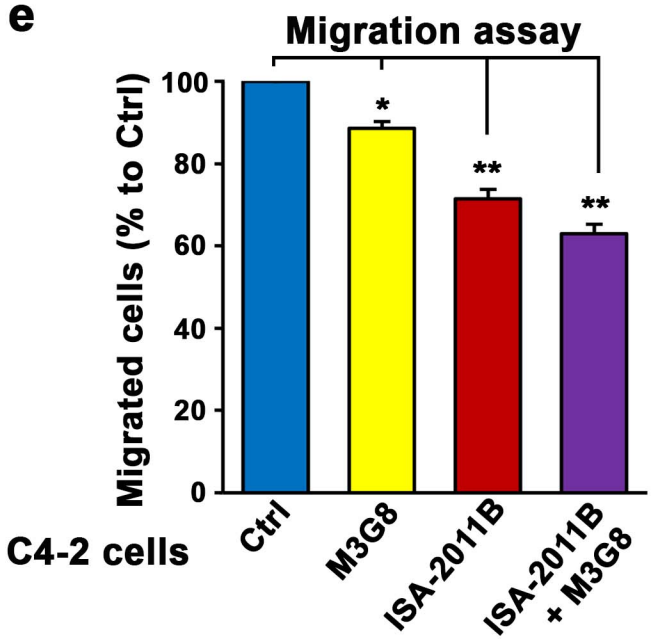
e
Migration assay
Migrated cells (% to Ctrl)
100
80
60
40
20
0
*
**
**
C4-2 cells
Ctrl
M3G8
ISA-2011B
ISA-2011B
+ M3G8